WRDC-TR-89-4053

EXPERIMENTAL EVALUATION OF NEW ALLOY COATINGS

Kang N. Lee and Wayne L. Worrell
University of Pennsylvania
Department of Materials Science
and Engineering
3231 Walnut Street
Philadelphia, PA 19104

July 1989

Final Report for Period November 86 - January 89

MATERIALS LABORATORY
WRIGHT RESEARCH DEVELOPMENT CENTER
AIR FORCE SYSTEMS COMMAND
WRIGHT-PATTERSON AIR FORCE BASE, OHIO 45433-6533

UNCLASSIFIED
SECURITY CLASSIFICATION OF THIS PAGE

REPORT DOCUMENTATION PAGE

Form Approved OMB No. 0704-0188

1a. REPORT SECURITY CLASSIFICATION Unclassified	1b. RESTRICTIVE MARKINGS
2a. SECURITY CLASSIFICATION AUTHORITY	3. DISTRIBUTION/AVAILABILITY OF REPORT Approved for public release; distribution is unlimited
2b. DECLASSIFICATION/DOWNGRADING SCHEDULE	
4. PERFORMING ORGANIZATION REPORT NUMBER(S)	5. MONITORING ORGANIZATION REPORT NUMBER(S) WRDC-TR-89-4053
6a. NAME OF PERFORMING ORGANIZATION University of Pennsylvania Dept. of Mat. Sci. & Eng. 6b. OFFICE SYMBOL (If applicable)	7a. NAME OF MONITORING ORGANIZATION Materials Laboratory (WRDC/MLBC) Wright Research and Development Center
6c. ADDRESS (City, State, and ZIP Code) 3231 Walnut Street Philadelphia PA 19104	7b. ADDRESS (City, State, and ZIP Code) Wright-Patterson AFB OH 45433-6533
8a. NAME OF FUNDING/SPONSORING ORGANIZATION Wright Research & Development Ctr Materials Laboratory 8b. OFFICE SYMBOL (If applicable) WRDC/MLBC	9. PROCUREMENT INSTRUMENT IDENTIFICATION NUMBER F33615-86-C-5138
8c. ADDRESS (City, State, and ZIP Code) Wright-Patterson AFB OH 45433-6533	10. SOURCE OF FUNDING NUMBERS PROGRAM ELEMENT NO. 62102F; PROJECT NO. 2417; TASK NO. 01; WORK UNIT ACCESSION NO. 24
11. TITLE (Include Security Classification) Experimental Evaluation of New Alloy Coatings	
12. PERSONAL AUTHOR(S) Kang N. Lee and Wayne L. Worrell	
13a. TYPE OF REPORT Final	13b. TIME COVERED FROM 11/86 TO 1/89
14. DATE OF REPORT (Year, Month, Day) 89 Jul 19	15. PAGE COUNT 45
16. SUPPLEMENTARY NOTATION	

17. COSATI CODES		
FIELD	GROUP	SUB-GROUP
11	02	00
11	04	00

18. SUBJECT TERMS (Continue on reverse if necessary and identify by block number)
Oxidation; Iridium; Aluminum; Hafnium; Silicon; Rhenium; Tungsten; Molybdenum; Oxidation Kinetics

19. ABSTRACT (Continue on reverse if necessary and identify by block number)

The oxidation behavior of binary iridium-aluminum and iridium-hafnium alloys, and ternary iridium-aluminum-silicon, rhenium-aluminum-silicon, tungsten-aluminum-silicon and molybdenum-aluminum-silicon alloys has been investigated in 1 atm oxygen at 1550°C (2822°F) - 1800°C (3272°F). Iridium-hafnium alloys form a protective hafnia scale at above 50 at% hafnium and iridium-aluminum alloys form a protective alumina scale at above 55 at% aluminum. Silicon decreases the aluminum concentration necessary for the formation of a protective alumina scale on iridium-aluminum alloys from around 55 to below 30 at%, and remarkably extends the lifetime of the alumina scale. Rhenium-aluminum-silicon, tungsten-aluminum-silicon, and molybdenum-aluminum-silicon alloys also exhibit good oxidation resistance, but the data are too sparse for any definite analysis or conclusions. The iridium-aluminum-silicon alloys with the aluminum concentration from 30 to 50 and the silicon concentration from 8 to 15 at% are proposed to be the best potential coating materials.

20. DISTRIBUTION/AVAILABILITY OF ABSTRACT ☒ UNCLASSIFIED/UNLIMITED ☐ SAME AS RPT. ☐ DTIC USERS	21. ABSTRACT SECURITY CLASSIFICATION Unclassified
22a. NAME OF RESPONSIBLE INDIVIDUAL STEPHEN L. SZARUGA	22b. TELEPHONE (Include Area Code) (513) 255-9059 22c. OFFICE SYMBOL WRDC/MLBC

DD Form 1473, JUN 86 *Previous editions are obsolete.*

SECURITY CLASSIFICATION OF THIS PAGE
UNCLASSIFIED

TABLE OF CONTENTS

Section		Page
I.	INTRODUCTION	1
II.	EXPERIMENTAL	3
III.	RESULTS AND DISCUSSION	
	Part I. Oxidation of Binary Alloys	5
	Part II. Oxidation of Ternary Alloys	21
IV.	SUMMARY	39
V.	CONCLUSIONS	42
	REFERENCES	44

List of Figures

Figure 1. The variation of weight change (TGA: for the Ir-50 and 65 at% Hf alloys; WGM: for the Ir and Ir-5 at% Hf alloy) with time for the oxidation of iridium-hafnium alloys exposed to 1 atm oxygen at 1,550°C. ---------- 6

Figure 2. SEM showing the cross section of the oxide scale formed on an iridium-50 at% hafnium alloy exposed to 1 atm oxygen for 2 hours at 1,550°C. ---------- 7

Figure 3. SEM showing the cross section of the oxide scale formed on an iridium-65 at% hafnium alloy exposed to 1 atm oxygen for 4 hours at 1,550°C.---------- 7

Figure 4. The variation of weight change (TGA) with time for the oxidation of an iridium-65 at% hafnium alloy exposed to 1 atm and 0.2 atm oxygen at 1,550°C. ---------- 9

Figure 5. The variation of $[\text{weight change}]^2$ with time for the oxidation of an iridium-65 at% hafnium alloy exposed to 1 atm and 0.2 atm oxygen at 1,550°C. ---------- 10

Figure 6. Calculated phase diagram for iridium-aluminum.[10] -------- 12

Figure 7. SEM showing the microstructure of an iridium-60 at% aluminum alloy (unetched).---------- 13

Figure 8. SEM showing the microstructure of an iridium-65 at% aluminum alloy (unetched).---------- 13

Figure 9. The variation of weight change (TGA: for the Ir-60 and 65 at% Al alloys; WGM: for the Ir and Ir-5, 22, 50, and 55 at% Al alloys) with time for the oxidation of iridium-aluminum alloys exposed to 1 atm oxygen at 1,650°C. ---------- 16

Figure 10. SEM showing the cross section of the oxide scale formed on an iridium-50 at% aluminum alloy exposed to 1 atm oxygen for 3 hours at 1,650°C. ---------- 17

Figure 11. SEM showing the cross section of the oxide scale formed on an iridium-65 at% aluminum alloy exposed to 1 atm oxygen for 48 hours at 1,600°C. ---------- 17

Figure 12. The variation of Log(parabolic-rate constant) with temperature for the oxidation of an iridium-60 at% aluminum alloy exposed to 1, 0.1 and 0.01 atm oxygen. --- 18

Figure 13. The variation of weight change (TGA) with time for the oxidation of iridium-aluminum-silicon alloys exposed to 1 atm oxygen at 1,550°C and 1,600°C.---------- 22

Figure 14. The variation of weight change (TGA) with time for the oxidation of an iridium-50 at% aluminum-8 at% silicon alloy exposed to 1 atm oxygen at 1,600°C.---------- 23

Figure 15. SEM showing the cross section of the oxide scale formed on an iridium-50 at% aluminum-8 at% silicon alloy exposed to 1 atm oxygen for 5 minutes at 1,600°C. - 26

Figure 16. SEM showing the cross section of the oxide scale formed on an iridium-50 at% aluminum-8 at% silicon alloy exposed to 1 atm oxygen for 1,000 hours at 1,600°C. ---------- 27

Figure 17. SEM showing the cross section of the oxide scale formed on an iridium-30 at% aluminum-10 at% silicon alloy exposed to 1 atm oxygen for 45 hours at 1,550°C. ---------- 28

Figure 18. SEM showing the cross section of the oxide scale formed on an iridium-30 at% aluminum-10 at% silicon alloy exposed to 1 atm oxygen for 380 hours at 1,550°C. ---------- 29

Figure 19. The variation of weight change (WGM) with time for the oxidation of rhenium-aluminum-silicon alloys exposed to 1 atm oxygen at 1,550°C.---------- 32

Figure 20. The variation of weight change (WGM) with time for the oxidation of tungsten-aluminum-silicon alloys exposed to air at 1,550°C.---------- 33

Figure 21. The variation of weight change (WGM) with time for the oxidation of molybdenum-aluminum-silicon alloys exposed to 1 atm oxygen at 1,550°C.---------- 34

Figure 22. The variation of weight change (WGM) with time for the oxidation of molybdenum-aluminum-silicon alloys exposed to 1 atm oxygen at 1,550°C.---------- 35

Figure 23. SEM showing the cross section of the oxide scale formed on a molybdenum-40 at% aluminum-30 at% silicon alloy exposed to 1 atm oxygen for 800 hours at 1,550°C. ---------- 37

Figure 24. SEM showing the cross section of the oxide scale formed on a molybdenum-30 at% aluminum-40 at% silicon alloy exposed to 1 atm oxygen for 800 hours at 1,550°C. ---------- 38

I. INTRODUCTION

The need for materials capable of sustained use in oxidizing environments at high temperatures has created much interest in the oxidation resistance of high-melting metals and alloys. Unfortunately, most of the refractory metals or alloys show poor oxidation resistance in oxidizing environments at high temperatures. However, a metal or an alloy may be protected from oxidation by coating.

After an extensive review of possible high-temperature metals and refractory compounds, we have selected iridium-base alloys as the most promising protective coating materials at ultrahigh temperatures. Iridium has a high melting point and exhibits relatively low oxidation rates compared to other high-melting metals. However, iridium forms gaseous oxides of IrO_2 and IrO_3 instead of a protective oxide scale in high-temperature oxidizing environments. Binary alloys in iridium-aluminum or iridium-hafnium systems could form external oxide layers if the concentration of aluminum or hafnium is large enough. The formation of a continuous external layer of Al_2O_3 or HfO_2 could prevent the formation of gaseous iridium oxides. Indeed previous studies of alumina-forming alloys[1-9] have shown that Al_2O_3 is one of the most effective barriers for high-temperature oxidation resistance.

In a binary alloy A-B, where element B is less noble than element A, the formation of a continuous external B oxide scale depends on the difference between the solubility-diffusivity product of oxygen and element B in the alloy. The alloy will form

a continuous external B oxide scale when $D_B C_B >> D_O C_O$ where D_B and D_O are the diffusivities of element B and oxygen in the alloy respectively, C_B is the concentration of element B, and C_O is the solubility of oxygen in the alloy. We well know that a third element C can lower the concentration of element B necessary for the formation of a continuous external B oxide scale.[10] For example, chromium significantly decreases the aluminum concentration necessary for the formation of a protective alumina scale in nickel-aluminum alloys.[2-5] Thus, it is possible that silicon could decrease the aluminum concentration necessary for the formation of a protective alumina scale in the binary aluminum alloys of iridium, rhenium, molybdenum, and tungsten.

This study investigates the development and growth of Al_2O_3 and HfO_2 scale on iridium-aluminum and iridium-hafnium alloys and the effect of silicon on the oxidation behavior of various alumina-forming binary alloys such as iridium-aluminum, rhenium-aluminum, molybdenum-aluminum, and tungsten-aluminum alloys. The optimum alloy coating compositions for oxidation protection between 1,550°C (2,822°F) and 1,800°C (3,272°F) in oxidizing environments have been determined.

II. EXPERIMENTAL

Interrupted weight-change measurements (WGM) and thermogravimetric-analysis (TGA) experiments have been used to investigate the oxidation kinetics. In TGA experiments, weight changes during oxidation have been continuously measured using a Cahn model 2000 electrobalance.

Iridium-base alloys containing a wide range of aluminum or hafnium and Iridium, rhenium, molybdenum, and tungsten-base alloys containing a wide range of aluminum and silicon were prepared by arc melting predetermined amounts of the pure metals. Specimens for the weight-change measurements were cut from the alloy coupons with a diamond saw. The specimens were then polished through 600 grit SiC paper, cleaned in an ultrasonic cleaner, and rinsed in acetone.

For a TGA experiment, a polished specimen was placed in a specially machined alumina holder, which was inserted into the furnace at the reaction temperature, and then hung from the balance using a sapphire fiber. To prevent any oxidation during the sample hanging process, the gas-tight alumina reaction tube was purged with an argon/5% hydrogen gas mixture, which was purified using titanium sponge at 800°C. After the balance was stabilized, the reaction gas of desired composition was passed through the reaction tube, and weight changes were monitored continuously using a strip-chart recorder with an accuracy of $\pm 10^{-4}$ g. For an interrupted weight-change measurement (WGM), a similar process was used except that a polished specimen was held in the reaction zone using an alumina crucible. The specimen was

then pulled out after a certain period of time, and the weight change was measured using a Mettler HL 52 electrobalance with an accuracy of $\pm 10^{-5}$ g.

After the oxidation experiments, selected specimens were sputter coated with gold, electroplated with copper, and pressure mounted with copper. The mounted specimens were polished through 0.25-micron diamond paste, coated with carbon, and then examined and characterized using scanning electron microscopy (SEM) and energy dispersive x-ray analysis (EDAX). For selected specimens, x-ray diffraction was used to determine the oxide phases present in the scale.

III. RESULTS AND DISCUSSION

Part I. Oxidation of Binary Alloys

Oxidation of Iridium-Hafnium Alloys

The oxidation kinetics of iridium-hafnium alloys containing 5, 50, and 65 at% hafnium have been investigated. Our x-ray diffraction results are in agreement with the iridium-hafnium phase diagram[11]. The iridium-50 at% hafnium alloy is an intermetallic compound HfIr, while the iridium-5 and -65 at% hafnium alloys are two-phase mixtures of hafnium-Hf_2Ir and HfIr-$HfIr_3$, respectively.

In Fig. 1, the observed weight changes for iridium-hafnium alloys exposed to 1 atm oxygen at 1,550°C are compared with that of pure iridium. The weight changes were measured using TGA for the iridium alloys containing 50 and 65 at% hafnium and using WGM for the iridium-5 at% hafnium alloy and pure iridium. Iridium and the iridium-5 at% hafnium alloy exhibit rapid weight losses because of the formation of gaseous iridium oxides. The iridium alloys containing 50 and 65 at% hafnium gain weight initially but eventually lose weight. The initial weight gain period increases as the hafnium content increases. SEM micrographs of the oxide scales for the iridium alloys containing 50 and 65 at% hafnium are shown in Figs. 2 and 3, respectively. The outer oxide layer (about 5 μm) of the iridium-65 at% hafnium alloy appears fairly dense (Fig. 3), while that of the iridium-50 at% hafnium alloy is very porous (Fig. 2). Apparently, the iridium alloys containing 50 and 65 at% hafnium initially form a protective external oxide layer. The selective oxidation of hafnium in the alloys

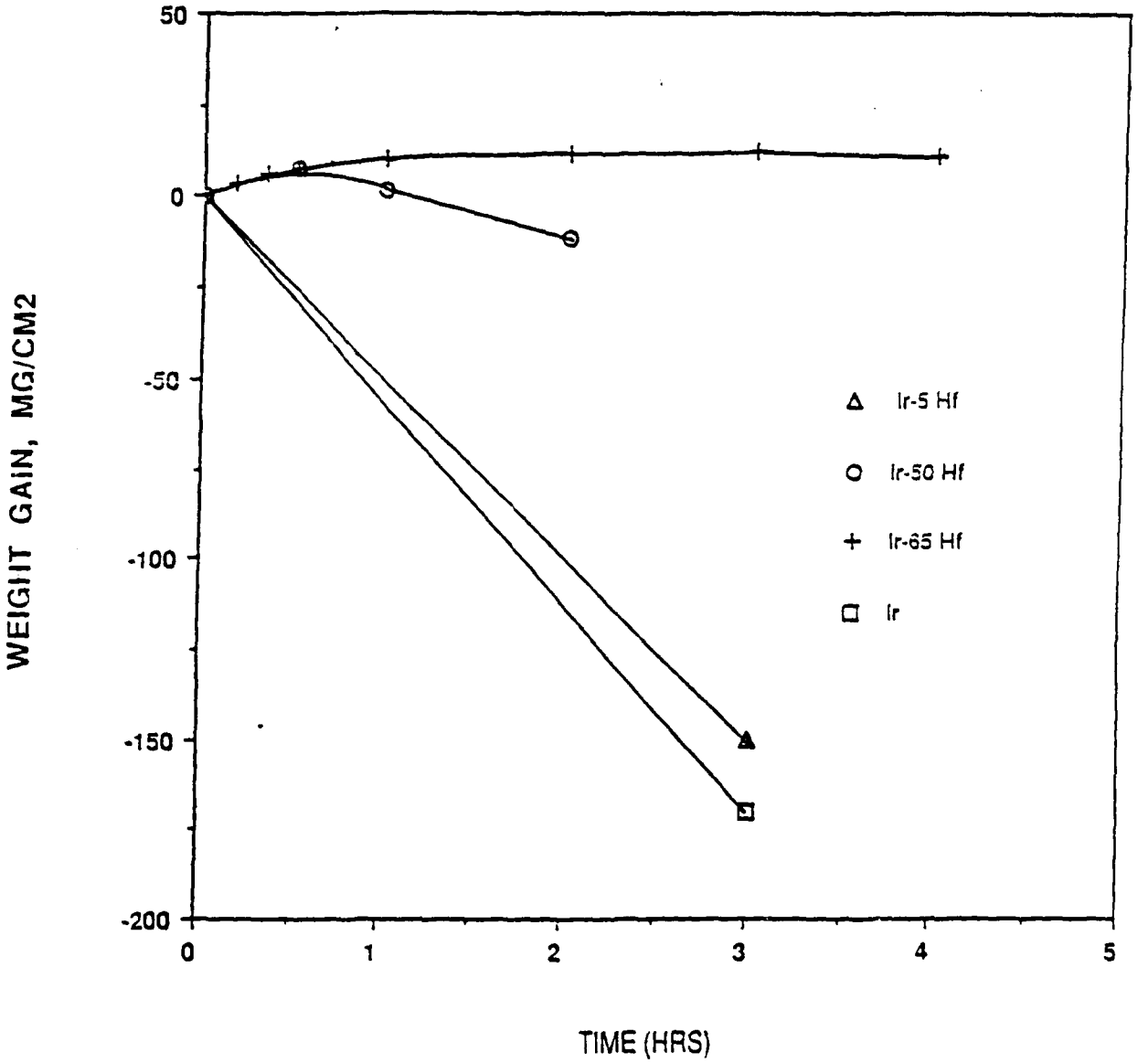

Figure 1. The variation of weight change (TGA: for the Ir-50 and 65 at% Hf alloys; WGM: for the Ir and Ir-5 at% Hf alloy) with time for the oxidation of iridium-hafnium alloys exposed to 1 atm oxygen at 1,550°C.

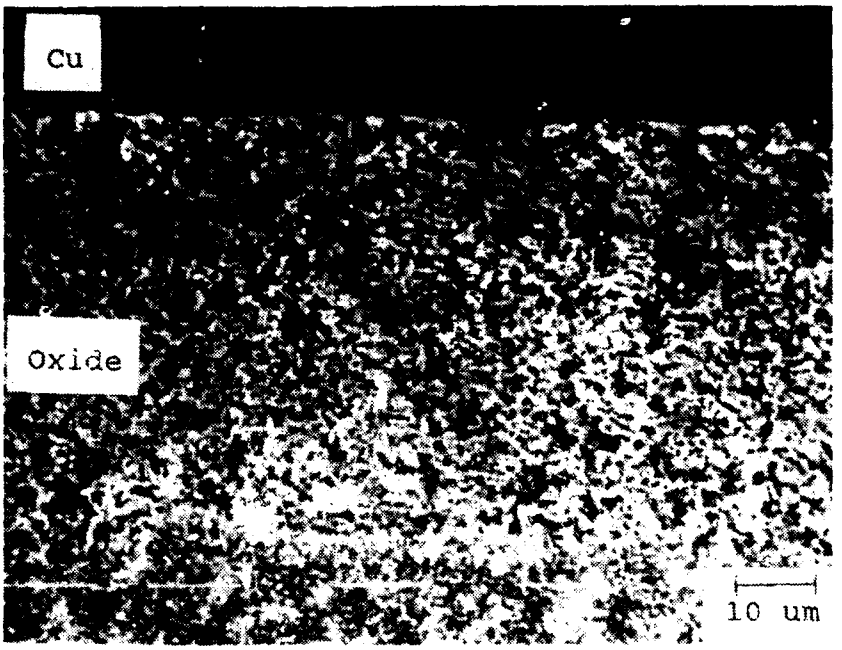

Figure 2. SEM showing the cross section of the oxide scale formed on an iridium-50 at% hafnium alloy exposed to 1 atm oxygen for 2 hours at 1,550°C.

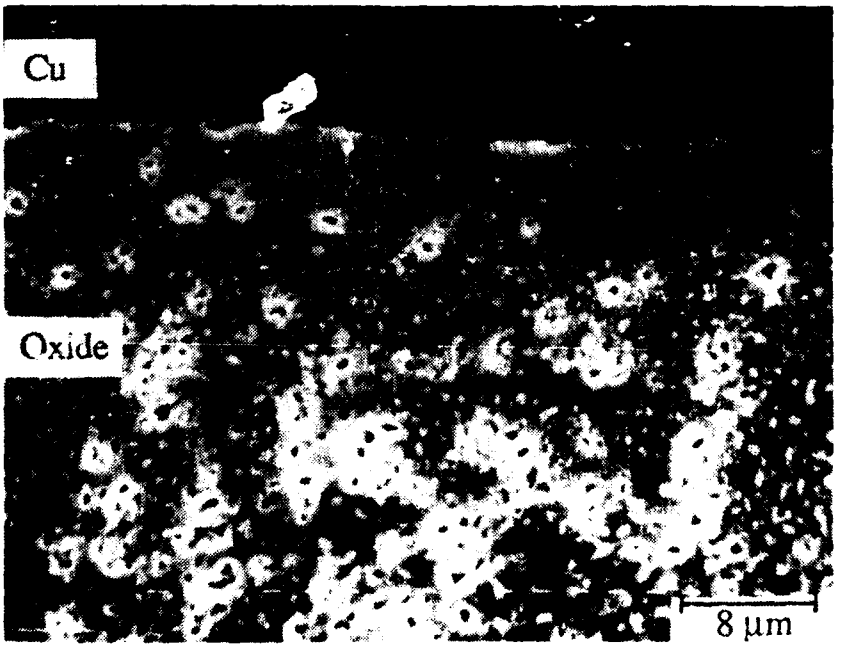

Figure 3. SEM showing the cross section of the oxide scale formed on an iridium-65 at% hafnium alloy exposed to 1 atm oxygen for 4 hours at 1,550°C.

eventually reduces the hafnium concentration below that necessary for the formation of a protective HfO_2 scale, and eventually a weight loss is observed as shown for the iridium-50 at% hafnium alloy in Fig. 1. Figure 4 shows the weight change curves measured using TGA for the iridium-65 at% hafnium alloy at 1,550°C exposed to 0.2 and 1 atm oxygen. After about 4 hours in 1 atm oxygen at 1,550°C, even the iridium-65 at% hafnium alloy loses weight. It is interesting to note that in 0.2 atm oxygen, the weight loss does not occur until after 8 hours.

Figure 5 indicates that the initial oxidation follows a parabolic-rate law and is independent of oxygen pressure. The dotted line is extrapolated from the previously determined parabolic-rate constant for pure hafnium.[12] Previous marker studies[13] suggest that the oxidation of hafnium is by the inward oxygen migration through the scale, and the parabolic-rate constant is independent of oxygen pressure at 800°C, which indicates that HfO_2 is an n-type oxide.

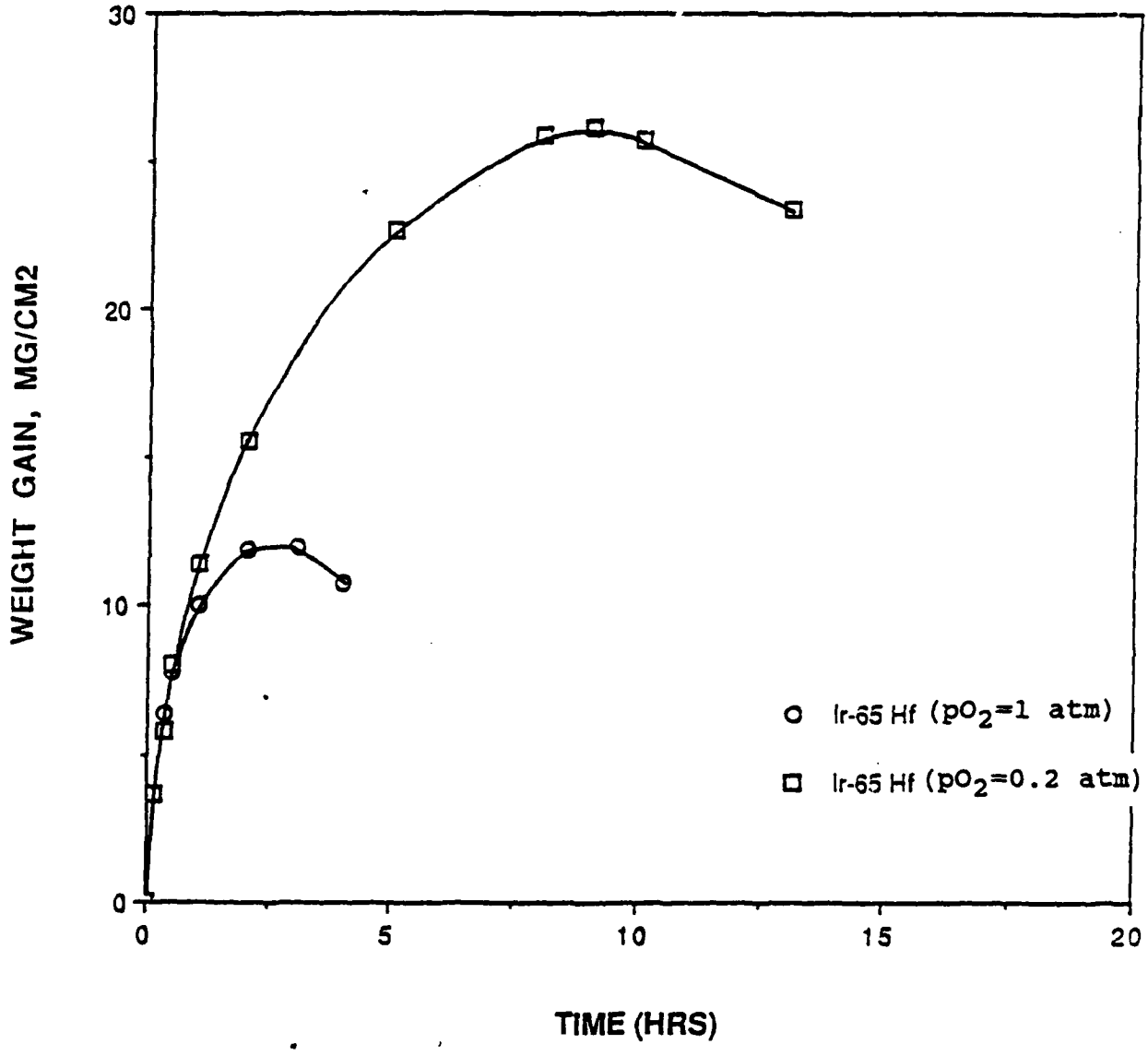

Figure 4. The variation of weight change (TGA) with time for the oxidation of an iridium-65 at% hafnium alloy exposed to 1 atm and 0.2 atm oxygen at 1,550°C.

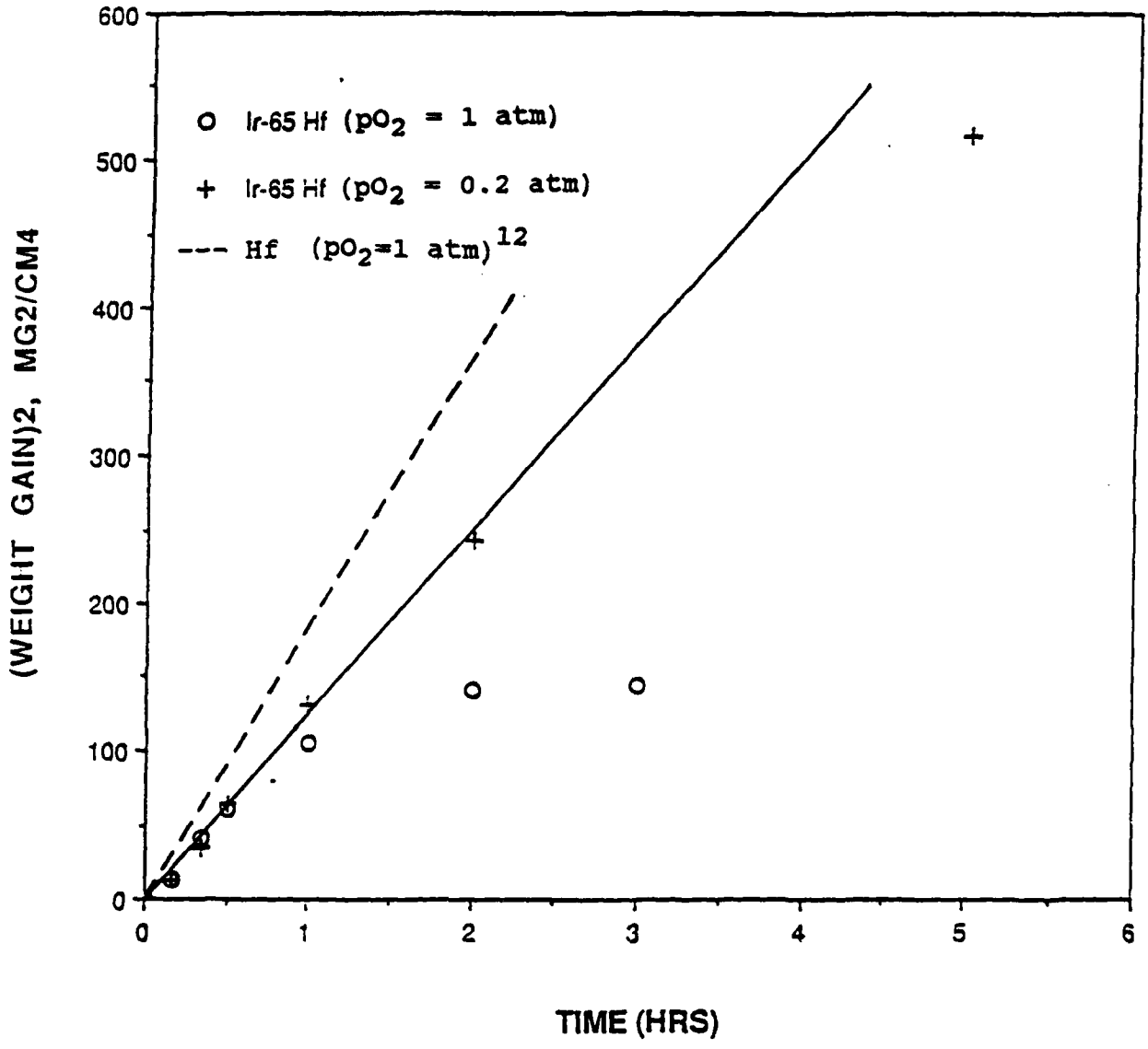

Figure 5. The variation of [weight change]^2 with time for the oxidation of an iridium-65 at% hafnium alloy exposed to 1 atm and 0.2 atm oxygen at 1,550°C.

Oxidation of Iridium-Aluminum Alloys

Our x-ray diffraction results for iridium-aluminum alloys containing 40, 55, 60, 65, 70, 72 and 74 at% aluminum are summarized in Table 1.

Table 1. X-ray Diffraction Results for Iridium-Aluminum Alloys.

Ir/Al (at%)	60/40	45/55	40/60	35/65	30/70	28/72	26/74
Phases	Ir +IrAl	IrAl	IrAl +$IrAl_{2.5}$	IrAl +$IrAl_{2.5}$	IrAl +$IrAl_{2.5}$	$IrAl_{2.5}$	$IrAl_3$ +$IrAl_{2.5}$

Although there is no reported phase diagram for the iridium-aluminum system, an estimated one[14] is shown in Fig. 6. Our studies indicate that the iridium-55 at% aluminum alloys exhibit an IrAl single phase. However, the iridium alloys containing 60, 65, 70 and 74 at% aluminum are two-phase mixtures. The microstructure for 60 and 65 at% aluminum alloys are shown in Figs. 7 and 8, respectively. The light phase contains about 55 - 57 at% aluminum, while the dark phase contains about 72 at% aluminum. X-ray diffraction confirms that the light phase is IrAl.[15] However, the diffraction patterns in the dark phase do not match the reported $IrAl_3$ peaks[15], even though Fig. 6 would suggest that the dark phase is $IrAl_3$. It is interesting to note that the $IrAl_3$ diffraction patterns are observed in the iridium-74 at% aluminum alloy. Any further characterization of the phase with about 72 at% aluminum is not possible from our results; thus the unknown phase is referred to as $IrAl_x$ ($x \approx 2.5$) in this report.

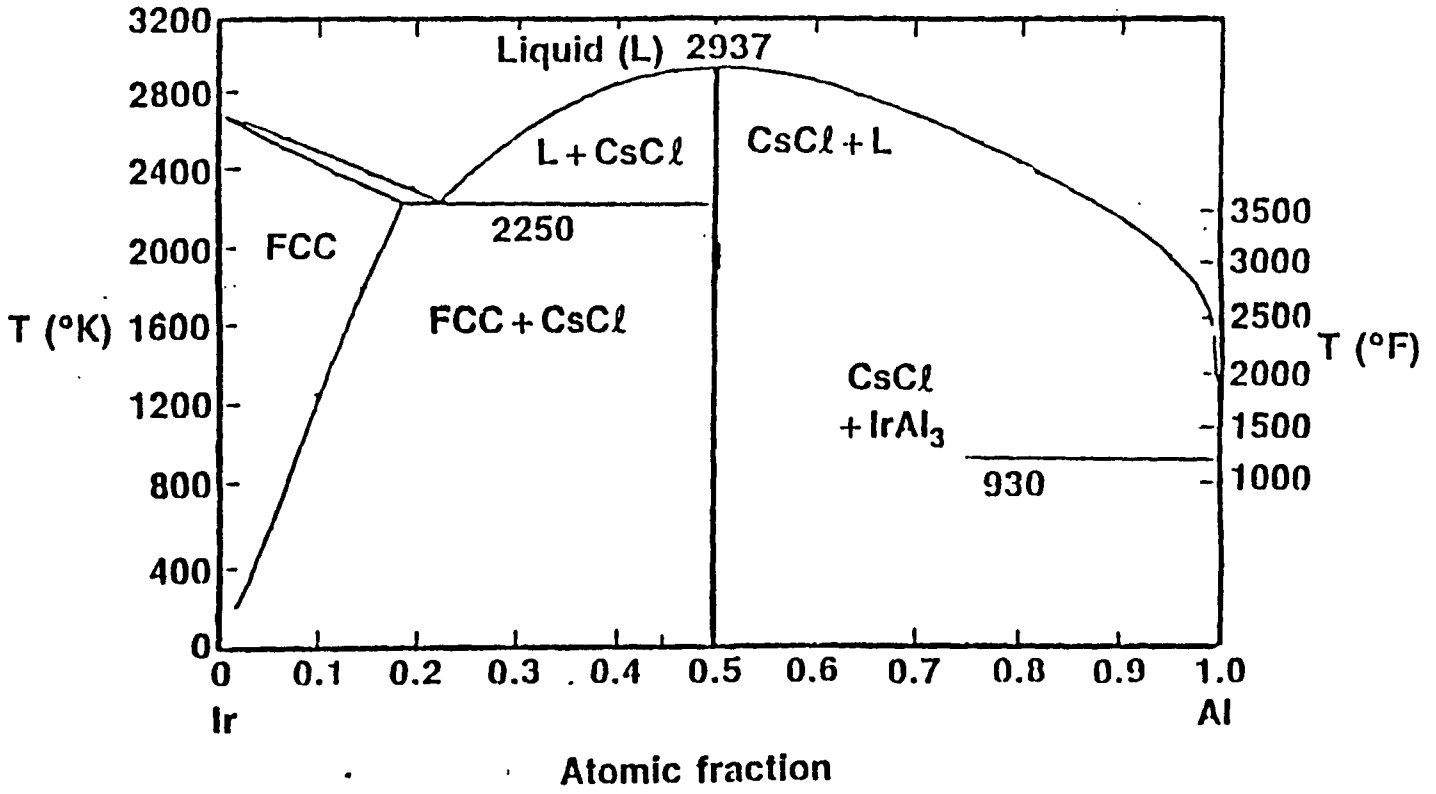

Fig. 6. Calculated phase diagram for iridium-aluminum.[10]

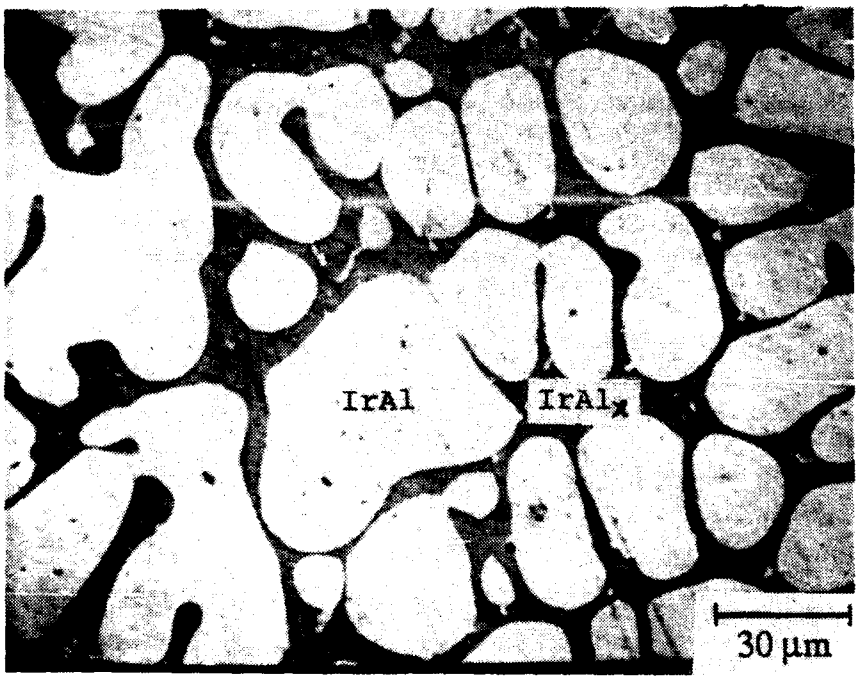

Figure 7. SEM showing the microstructure of an iridium-60 at% aluminum alloy (unetched).

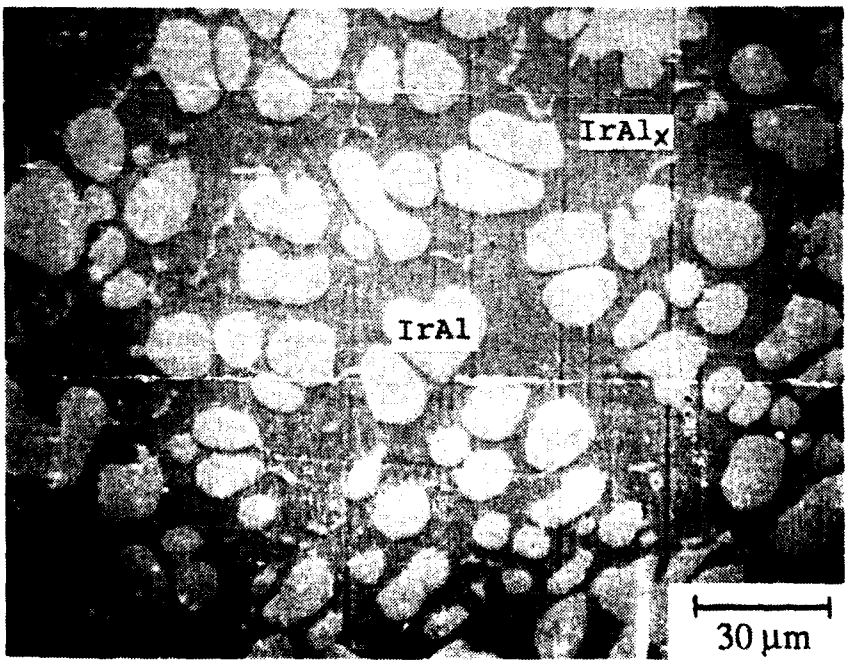

Figure 8. SEM showing the microstructure of an iridium-65 at% aluminum alloy (unetched).

The iridium-65 at% aluminum alloy shows partial melting at 1,650°C and above (no melting at 1,600°C and below), while the iridium-60 at% aluminum alloy does not show apparent melting at temperatures up to 1,800°C. The major proportion (≈ 74 mol%) of the iridium-60 at% aluminum alloy is the IrAl (Fig. 7), whereas the major proportion (≈ 58.4 mol%) of the iridum-65 at% aluminum alloy is the $IrAl_x$ (Fig. 8). Thus, we suggest that the melting temperature of the $IrAl_x$ ($x \approx 2.5$) is between 1,600 and 1,650°C and that of the IrAl is above 1,800°C. The iridium-60 at% aluminum alloy does not show apparent melting at temperatures above 1,650°C because the amount of liquid ($IrAl_x$) is small (≈ 26 mol%).

Iridium-aluminum alloys containing 5, 22, 50, 55, 60 and 65 at% aluminum have been oxidized in 1 atm oxygen at 1,650°C. The results shown in Fig. 9 indicate that alloys with 55 at% or less aluminum do not form a protective oxide scale and lose weight because of the formation of gaseous iridium oxides. The weight changes were measured using TGA for the iridium alloys containing 60 and 65 at% aluminum and using WGM for pure iridium and the iridium alloys containing 5, 22, 50 and 55 aluminum. As shown in Fig. 10, the oxide scale formed on the iridium-55 at% aluminum alloy is extremely porous; thus more than 55 at% aluminum is required to form a protective Al_2O_3 scale. As indicated earlier, 55 at% aluminum is the aluminum-rich boundary of the IrAl phase, which implies $IrAl_x$ ($x \approx 2.5$) is necessary for the formation of a protective Al_2O_3 scale. Indeed, Fig. 9 indicates that aluminum alloys containing 60 and 65 at% aluminum form a protective

external Al_2O_3 scale which prevents the formation of gaseous iridium oxides. The oxide scale formed on the iridium-65 at% aluminum alloy appears dense and protective (Fig. 11).

The activation energy for oxidation has been determined by oxidizing iridium-60 at% aluminum alloys at temperatures between 1,550 and 1,800°C and at oxygen pressures between 0.01 and 1 atm. Although a parabolic-rate law is observed, SEM has shown that the alloys lose some iridium because of a local breakdown of the protective oxide scale, particularly at temperatures above 1,700°C. To avoid any error from the loss of iridium, the thickness of the oxide scales is measured using the SEM micrographs, and rate constants are calculated from the measured thickness assuming 100% dense Al_2O_3. Results are shown in Fig. 12. Results[1] for the oxidation of NiAl from WGM at temperatures between 1,000 and 1,300°C are also included for comparison in Fig. 12. The oxidation of the iridium-60 at% aluminum alloy has the same activation energy (76 ± 5 kcal/mol) as that for NiAl. This agreement indicates that the growth of an Al_2O_3 scale controls the oxidation rate of these two alloys.

Scale-morphology studies[8,16] have indicated that Al_2O_3 grows by the inward migration of oxygen. Experiments with $^{16}O_2/^{18}O_2$ tracers for the growth of Al_2O_3 on NiCrAl alloys at 1,100°C[17] have shown that inward oxygen transport via grain-boundaries is the dominant transport process. The agreement in Fig. 12 suggests that inward oxygen transport via grain-boundary diffusion could also be the rate-limiting process for the oxidation of iridium-aluminum alloys. The oxygen diffusion coefficient in

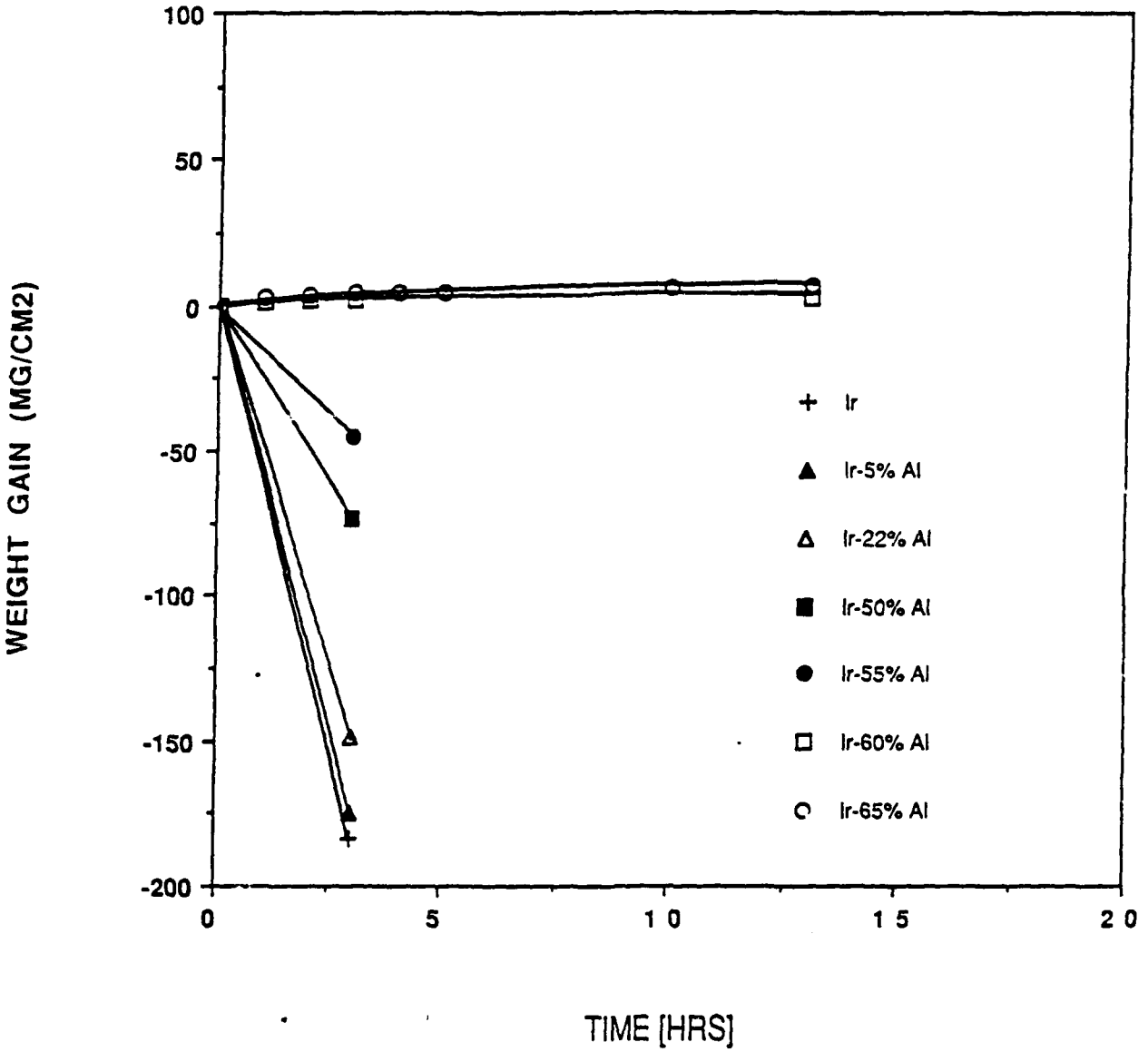

Figure 9. The variation of weight change (TGA: for the Ir-60 and 65 at% Al alloys; WGM: for the Ir and Ir-5, 22, 50, and 55 at% Al alloys) with time for the oxidation of iridium-aluminum alloys exposed to 1 atm oxygen at 1,650°C.

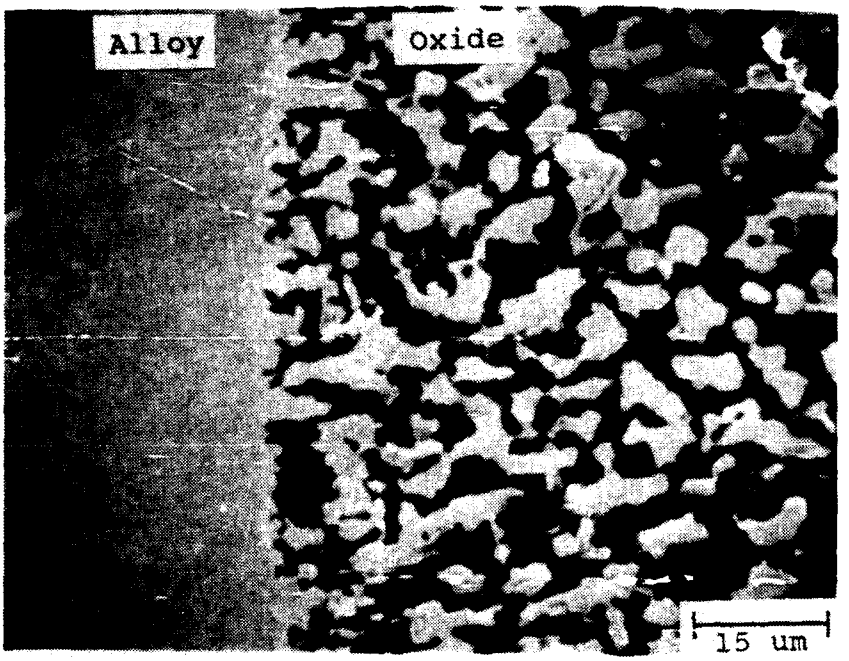

Figure 10. SEM showing the cross section of the oxide scale formed on an iridium-50 at% aluminum alloy exposed to 1 atm oxygen for 3 hours at 1,650°C.

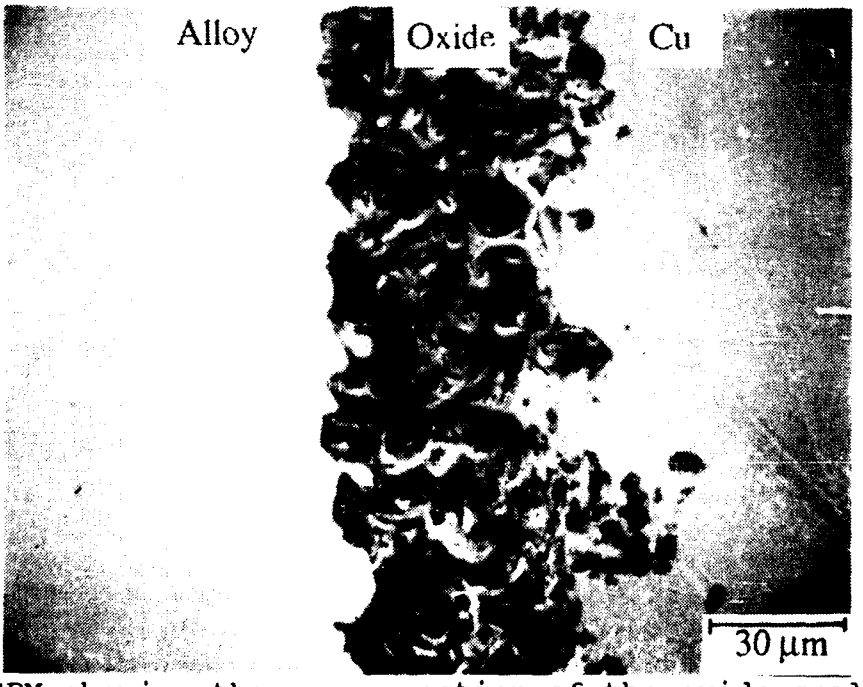

Figure 11. SEM showing the cross section of the oxide scale formed on an iridium-65 at% aluminum alloy exposed to 1 atm oxygen for 48 hours at 1,600°C.

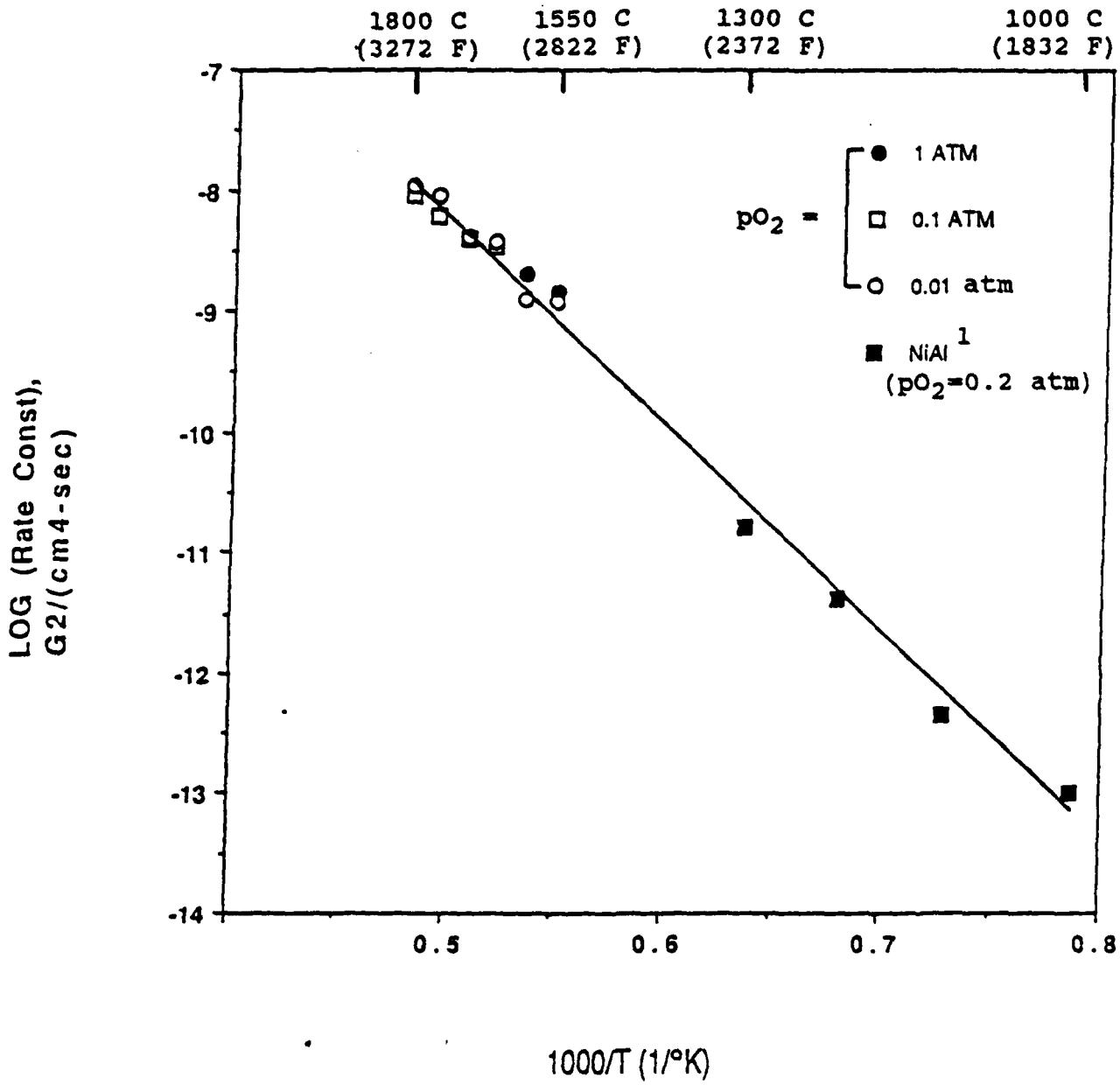

Figure 12. The variation of Log(parabolic-rate constant) with temperature for the oxidation of an iridium-60 at% aluminum alloy exposed to 1, 0.1 and 0.01 atm oxygen.

polycrystalline Al_2O_3 is nearly two orders of magnitude larger than that observed for single crystal Al_2O_3,[18] which is ascribed to enhanced grain-boundary diffusion. Above 1,450°C, the activation energy for oxygen diffusion in polycrystalline Al_2O_3 is 110 kcal/mol[18], which is significantly larger than the activation energy for Al_2O_3-scale growth in this study (76 ± 5 kcal). However, the grain size (130 μm) of their polycrystalline specimens is larger than the thickness (5 μm after 5 minutes and 50 μm after 48 hours) of the Al_2O_3 scales formed on our iridium-aluminum alloys at 1,600°C. The small grain size of our Al_2O_3 scales could enhance oxygen diffusion, and decrease the activation energy.

After 1 minute of oxidation, the oxide scale of an iridium-65 at% aluminum alloy exposed to 1 atm oxygen at 1,600°C is not continuous, and only the IrAl phase is observed near the alloy/scale interface. The absence of the $IrAl_x$ phase indicates an aluminum-depletion zone, presumably due to the slow transport of aluminum in the alloy. After 5 minutes of oxidation, the oxide scale is continuous, and oxygen must diffuse through the Al_2O_3 scale. Because oxygen diffusion through the scale is slower than the aluminum diffusion in the alloy, no aluminum-depletion zone at the scale/alloy interface is observed. After 48 hours of oxidation (Fig. 11), the Al_2O_3 scale is dense and continuous. The aluminum concentration of the alloy decreases as the oxidation continues, and the alloy becomes mostly IrAl. At this stage, if the Al_2O_3 scale cracks, a protective oxide scale will not form at the bottom of the crack because the aluminum concentration in the

alloy is below that necessary for the formation of a continuous Al_2O_3 scale. Thus, the alloy oxidizes rapidly by forming a porous Al_2O_3 scale and gaseous iridium oxides.

Part II. Oxidation of Ternary Alloys

Oxidation of Iridium-Aluminum-Silicon Alloys

The TGA results for iridium-aluminum-silicon alloys exposed to 1 atm oxygen are shown in Fig. 13. After around 60 hours, the iridium-60 aluminum alloy (20 mils thick) exhibits nonprotective oxidation and forms porous Al_2O_3 scales and gaseous iridium oxides presumably due to aluminum depletion in the alloy. However, the iridium-30 aluminum-10 silicon alloy (20 mils thick) shows protective oxidation behavior for almost 300 hours. To examine the adherence of the oxide scale formed on iridium-aluminum-silicon alloys, an iridium-50 aluminum-8 silicon alloy (42 mils thick) has been exposed to 1 atm oxygen and thermally cycled between 1,600 C and room temperature for 1,000 hours (Figs.13 and 14). In the temperature-cycling test, the alloy is pulled out of the furnace to room temperature in about 5 seconds, cooled down to room temperature, and inserted back to the furnace in about 5 seconds (arrows in Fig. 14). Thermal cycling does not lead to scale spallation or an increased oxidation rate. Thus, silicon decreases the aluminum concentration necessary for the formation of a protective alumina scale from around 55 to below 30 at%, and remarkably increases the lifetime of the oxide scale under thermal cycling. Although the data are not shown in this report, all iridium-aluminum-silicon alloys with 30 - 50 at% aluminum and 8 - 15 at% silicon show a protective oxidation behavior with considerably longer lifetime compared with that of iridium-aluminum binary alloys.

The dotted line in Fig. 14 is the extrapolated oxidation behavior for an iridium-65 aluminum alloy at 1,600°C in 1 atm

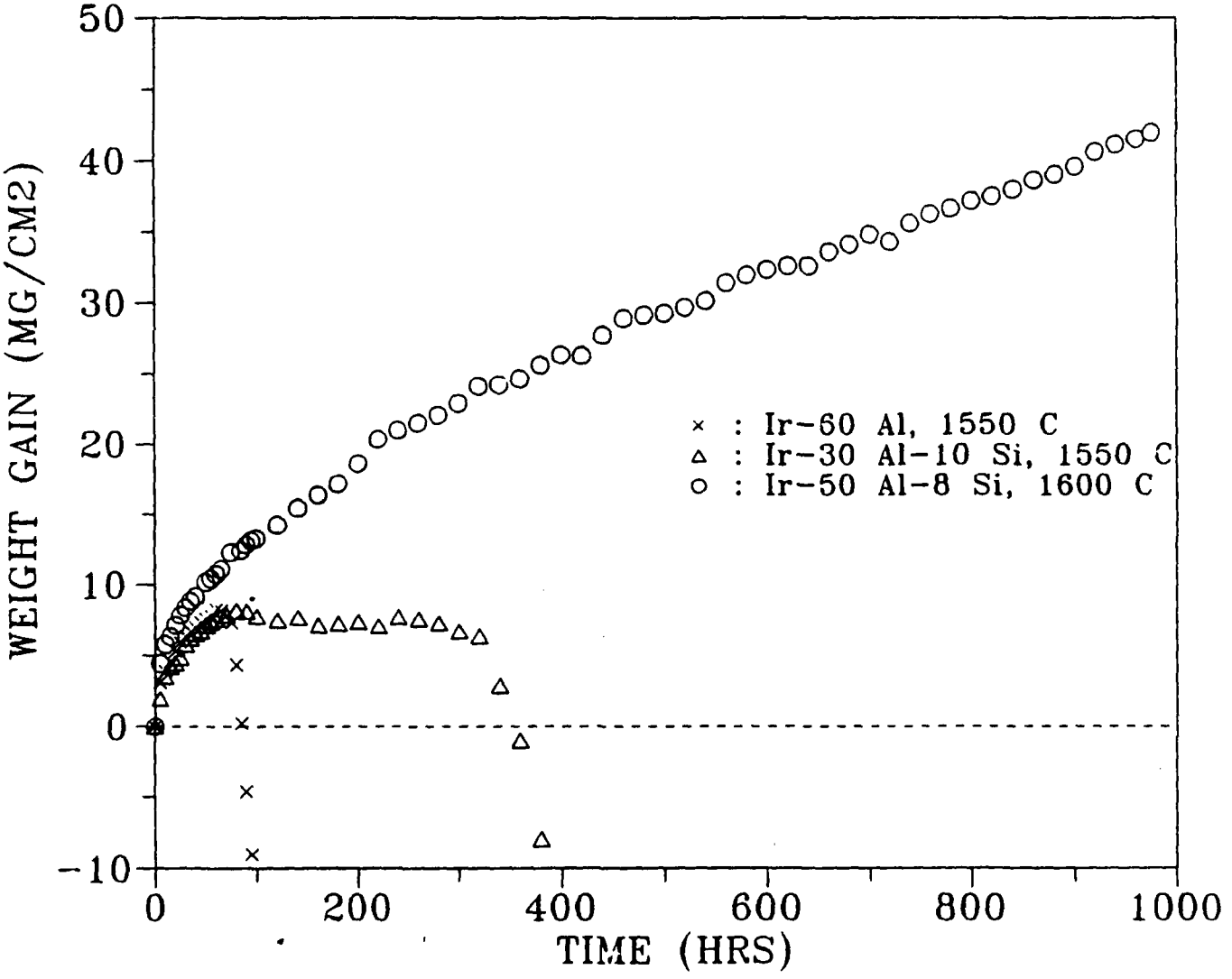

Figure 13. The variation of weight change (TGA) with time for the oxidation of iridium-aluminum-silicon alloys exposed to 1 atm oxygen at 1,550°C and 1,600°C.

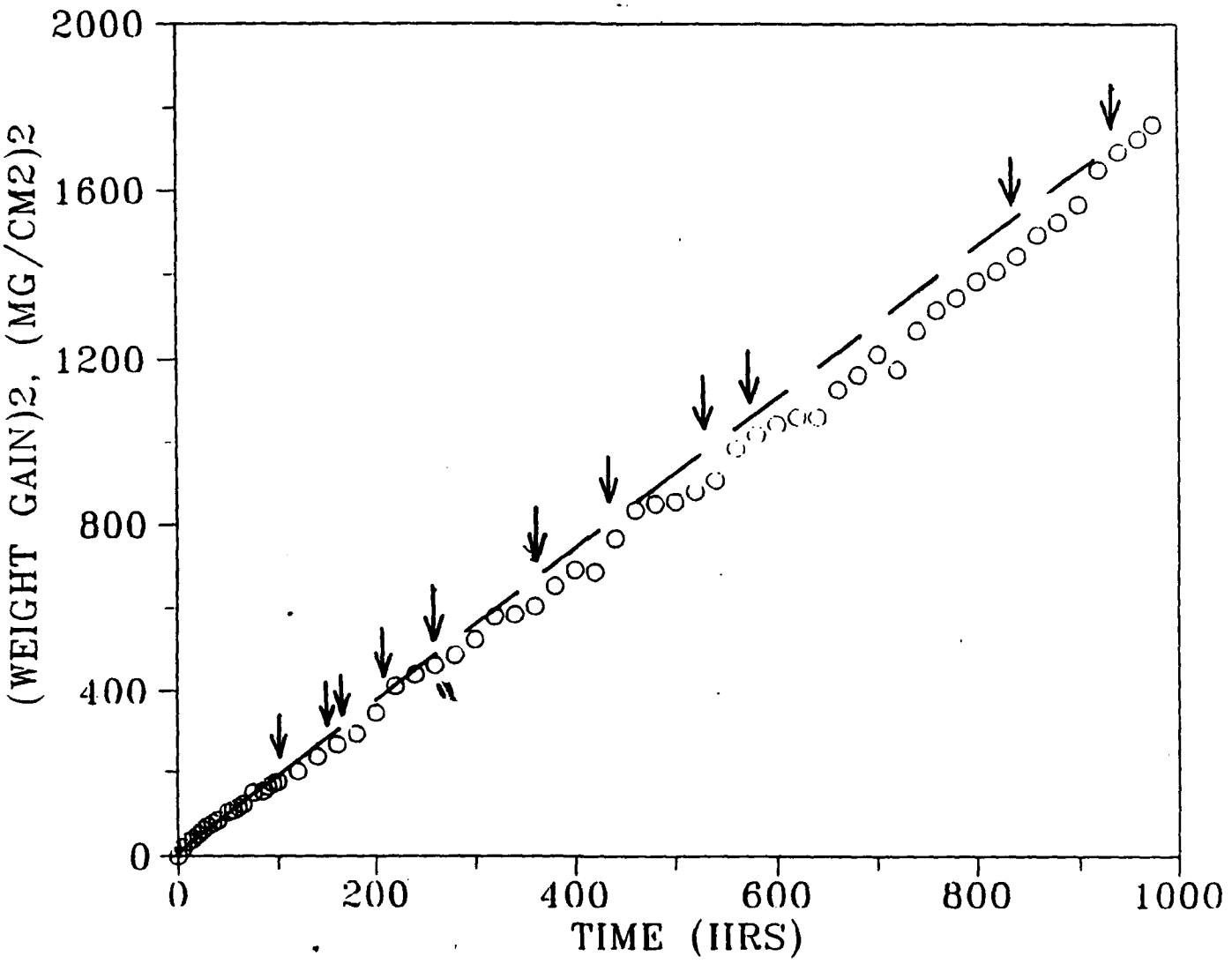

Figure 14. The variation of weight change (TGA) with time for the oxidation of an iridium-50 at% aluminum-8 at% silicon alloy exposed to 1 atm oxygen at 1,600°C.

oxygen. The overall oxidation kinetics of the ternary iridium-50 aluminum-8 silicon alloy follows a parabolic rate law, and the oxidation rate is about same as that for the binary iridium-65 aluminum alloy. Thus, it appears that the oxide scale is virtually pure alumina, continuous and protective.

Figures 15.a and 16.a show the cross sections of the oxide scale for an iridium-50 aluminum-8 silicon alloy after 5 minutes and 1,000 hours of oxidation, respectively, in pure oxygen at 1,600°C. Figures 15.b, 15.c, 16.b, and 16.c are EDAX maps of aluminum and silicon for the cross sections shown in Figs. 15.a and 16.a. Figure 15.a shows that after 5 minutes of oxidation, the oxide scale is continuous and contains some pores. Some porous alumina particles are found at the outer edge of the scale. The morphology of the oxide scale is very similar to that of the oxide scale formed on an iridium-65 aluminum alloy. EDAX analysis (Figs. 15.b, 15.c, 16.b, and 16.c) shows that there is no silicon in the oxide scale even after 1,000 hours of oxidation. Thus, the SEM/EDAX analysis and the oxidation kinetics indicate that the oxide scale is virtually pure alumina and that the oxidation is controlled by the growth rate of alumina. Because the equilibrium oxygen pressure for the coexistence of Al_2O_3/Al is about 5 orders of magnitude smaller than that for the coexistence of SiO_2/Si at 1600°C,[19] a silica scale does not form when the alumina scale is continuous and protective.

Figures 17.a and 18.a show the cross sections of the oxide scales on an iridium-30 aluminum-10 silicon alloy after 45 and 380 hours of oxidation, respectively, in pure oxygen at 1,550°C. EDAX

maps (Figs. 17.b and 17.c) show that there is no silicon in the oxide scale after 45 hours of oxidation. However, a layer of high silicon concentration is found at the inner edge of the oxide scale after 380 hours of oxidation (Fig. 18.c), when the oxide scale is no longer protective (see Fig. 13). Table 2 is the mol% of alumina and silica in the oxide scale at the locations shown by numbers 1 to 9 in Fig. 18.a.

Table 2. Molar percent of Al_2O_3 and SiO_2 in the oxide scale on an iridium-30 aluminum-10 silicon alloy shown in figure 18.a.

#	1	2	3	4	5	6	7	8	9
Al_2O_3	4.07	5.01	5.23	5.55	5.89	15.39	33.03	67.35	100
SiO_2	95.93	94.99	94.77	94.45	94.11	84.61	66.97	32.65	0

The inner layer with high silicon concentration is mostly a SiO_2-Al_2O_3 eutectic mixture (about 5 mol% Al_2O_3), and the fraction of Al_2O_3 increases in the scale to pure Al_2O_3 at the scale/gas interface.

When the aluminum activity at the alloy/oxide interface decreases to the value necessary for reaction (1) to proceed, SiO_2 will begin to form at the alloy/scale interface. This occurs after around 90 hours for the iridium-30 aluminum-10 silicon alloy at 1,550°C in 1 atm oxygen. The chemical stability of a SiO_2 or an Al_2O_3 layer on an alloy containing aluminum and silicon can be calculated from equation (1).

$$3/2\ \underline{Si} + Al_2O_3 = 3/2\ SiO_2 + 2\ \underline{Al} \qquad (1)$$

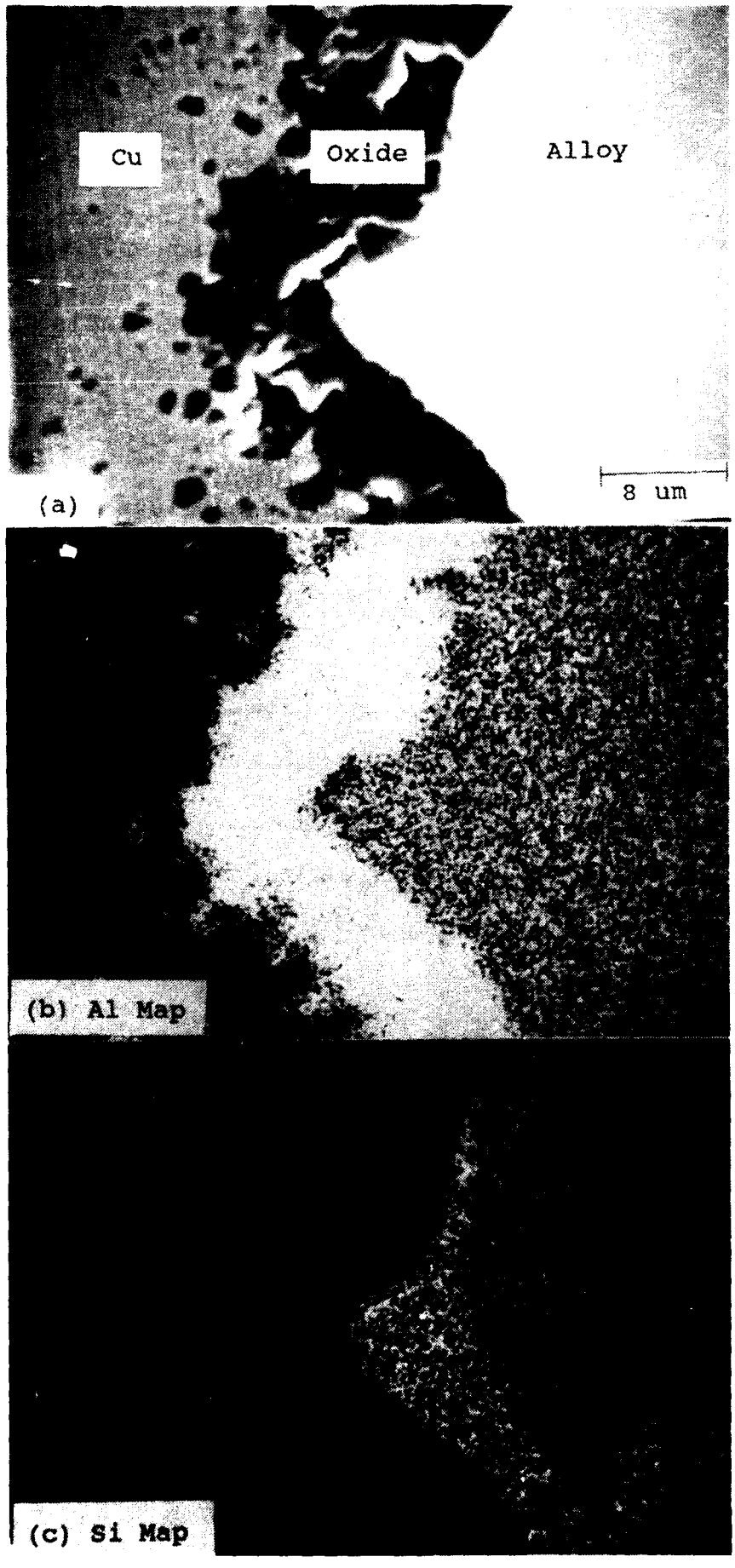

Fig. 15.
Ir-50 Al-8 Si
1 atm Oxygen
5 minutes
T= 1,600°C

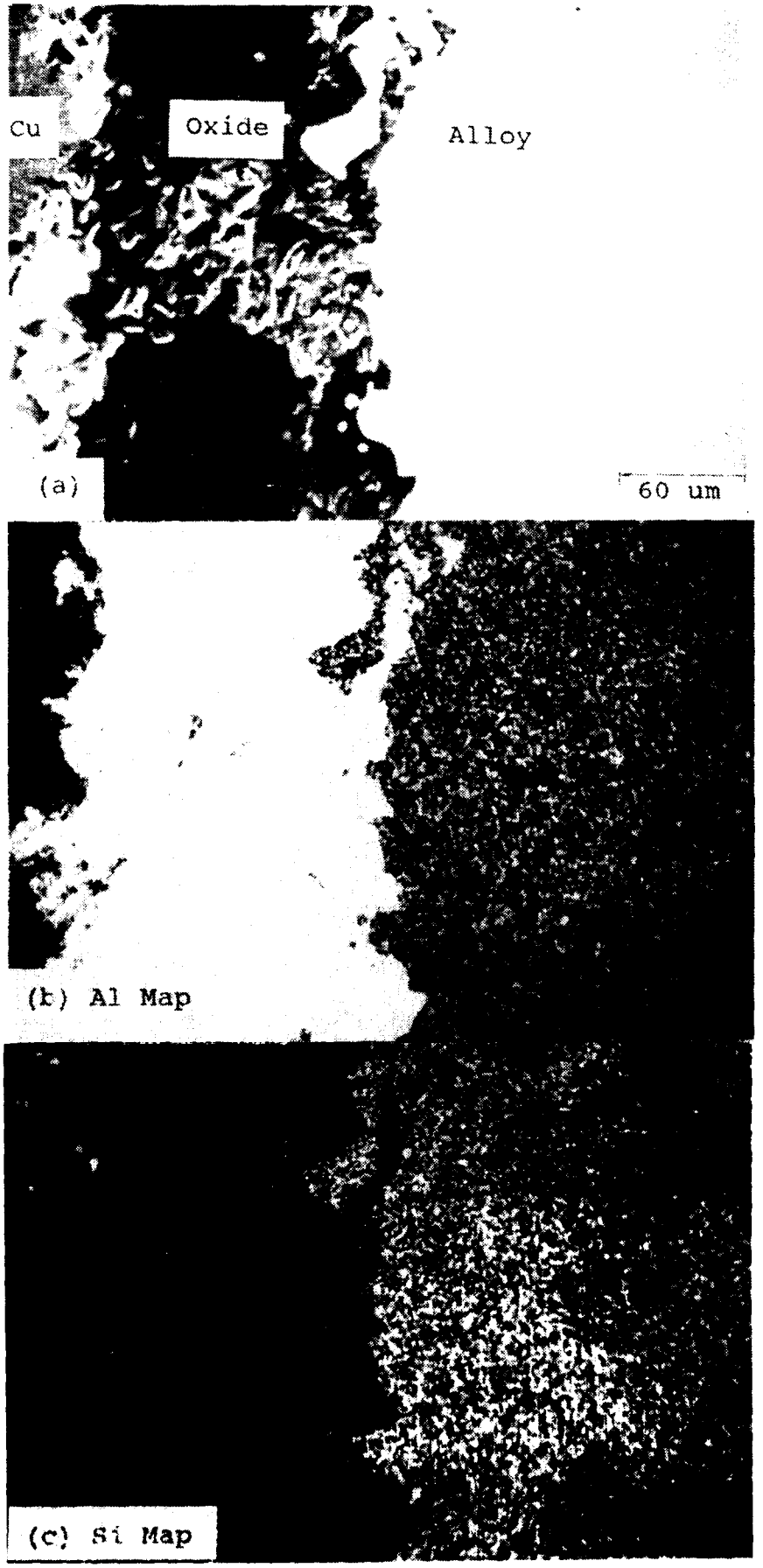

Fig. 16.
Ir-50 Al-8 Si
1 atm Oxygen
1,000 Hours
T= 1,600°C

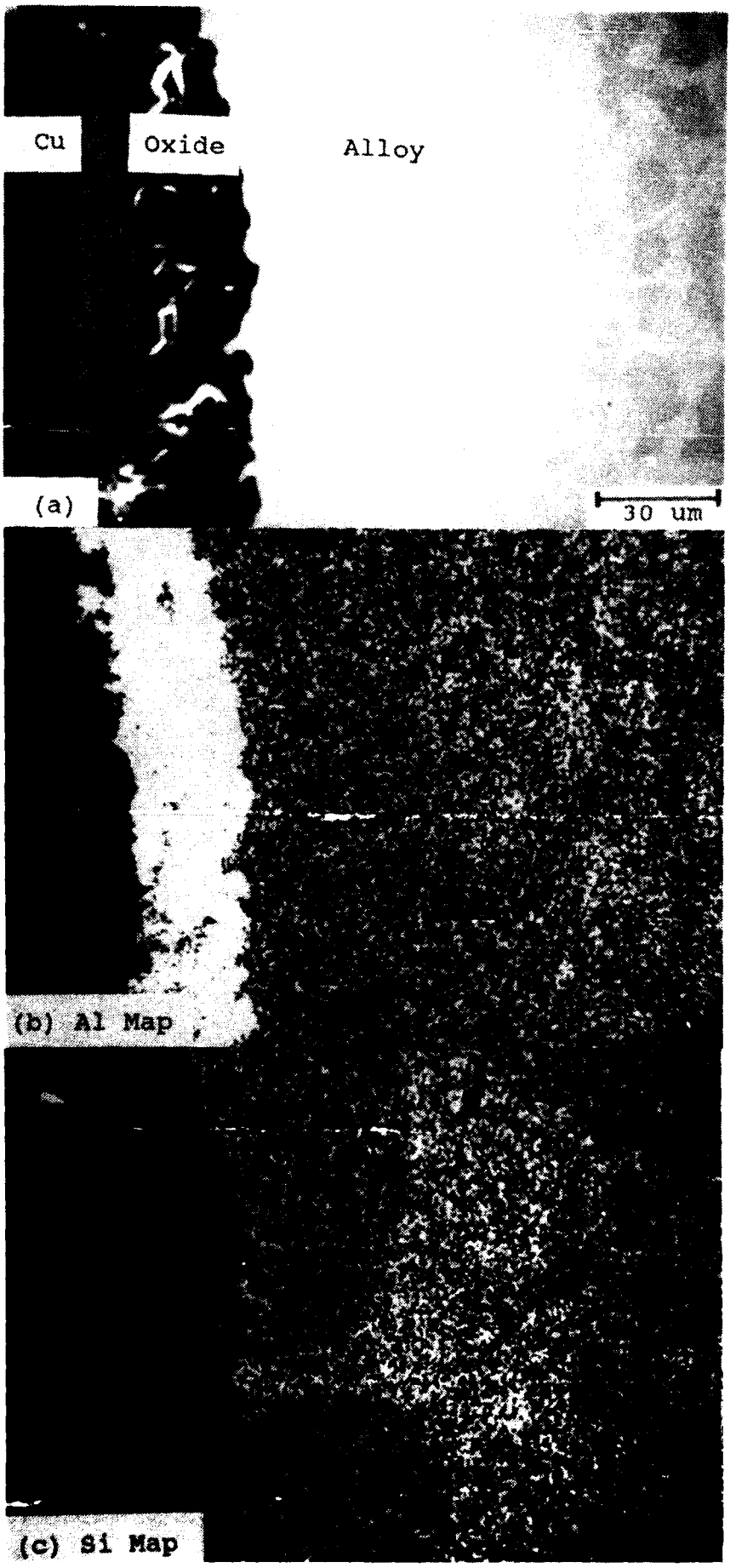

Fig. 17.
Ir-30 Al-10 Si
1 atm Oxygen
45 Hours
T= 1,550°C

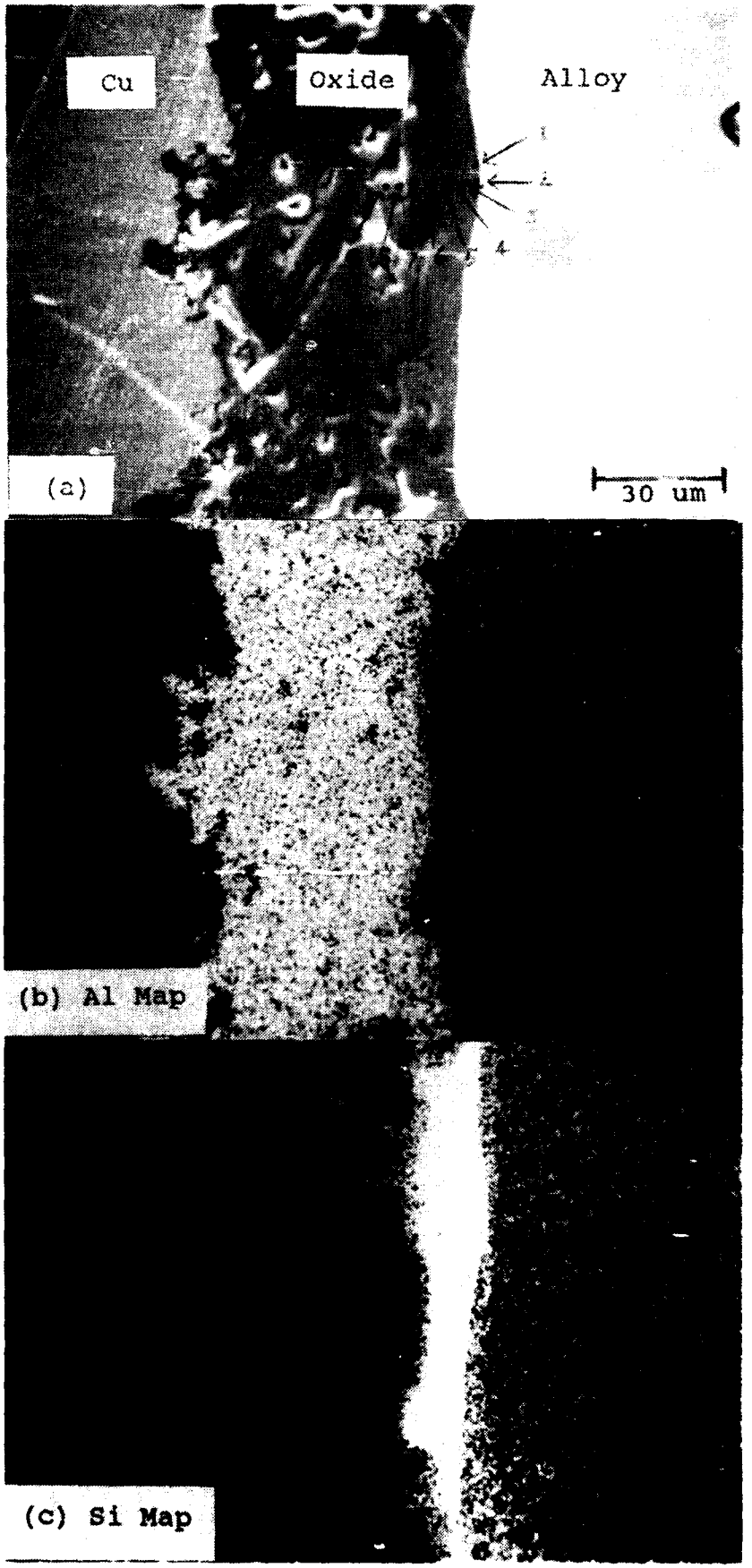

Fig. 18.
Ir-30 Al-10 Si
1 atm Oxygen
380 Hours
T= 1,550°C

The standard free energy for reaction (1) is 50,828 cal,[19] and the equilibrium constant is 8.05×10^{-7} at 1,550°C. Assuming that the silicon activity is equal to its mole fraction ($a_{Si} = 0.1$), equation (1) requires that the aluminum activity at the alloy/oxide interface is less than 5.05×10^{-3} before SiO_2 will form. The parabolic rate constant for the formation of silica is about 1.5 to 2 orders of magnitude smaller than that of alumina at 1,550°C.[20] Thus, the formation of an inner silica layer will decrease the oxidation rate significantly. The decreasing weight for the iridium-30 aluminum-10 silicon alloy after about 90 hours in Fig. 13 suggests that the alloy is losing iridium presumably due to scale cracking and that the rate of weight loss by the loss of iridium is slightly faster than that of weight gain by the formation of silica. In addition, the oxygen-activity gradient across the inner silica layer is extremely low. Thus the weight change is virtually negligible after about 90 hours of oxidation in Fig. 13. After about 320 hours, the activity of silicon in the alloy decreases below that necessary for the formation of a continuous silica layer, and the alloy loses weight rapidly due to the formation of volatile iridium oxides.

Oxidation of Rhenium-Aluminum-Silicon, Molybdenum-Aluminum-Silicon, and Tungsten-Aluminum-Silicon Alloys

Interrupted weight-change measurement (WGM) curves for rhenium-aluminum-silicon, tungsten-aluminum-silicon, and molybdenum-aluminum-silicon alloys (20 mils thick) exposed to 1 atm oxygen or air at 1,550°C are shown in Figs. 19, 20, and 21,

respectively. The rhenium-40 aluminum-30 silicon alloy in 1 atm oxygen at 1,550°C exhibits an initial weight gain followed by small weight loss, whereas the rhenium-30 aluminum-30 silicon alloy exhibits a rapid weight loss initially, which appears to decrease after around 25 hours. The sparse data (two points) for the tungsten-40 aluminum-30 silicon and the tungsten-30 aluminum-40 silicon alloys indicate that they gain weight during the first 24 hours in air at 1,550°C. The lack of any additional data for the rhenium and tungsten alloys preclude any definitive analysis and conclusions.

The molybdenum-40 aluminum-30 silicon, and molybdenum-30 aluminum-40 silicon alloys have been exposed to 1 atm oxygen, and thermally cycled between 1,550°C and room temperature. The data points in Fig. 21 represent the cycling times (the cooling and heating time during each cycle was about 10 min). After around 800 hours of oxidation, the molybdenum-40 aluminum-30 silicon alloy still exhibits a protective oxide scale. However, the molybdenum-30 aluminum-40 silicon alloy loses weight sometime between 500 and 800 hours (Fig. 21). There was no evidence of scale spallation in either alloy. Figure 22 is a plot of weight gain^2 vs time for the molybdenum-base alloys. The dotted line in Fig. 22 is the extrapolated oxidation behavior for the iridium-65 aluminum alloy at 1,550°C in 1 atm oxygen. Comparing the results for the molybdenum-aluminum-silicon alloys with the extrapolated line indicates that there is some loss of molybdenum presumably due to the formation of volatile molybdenum oxides.

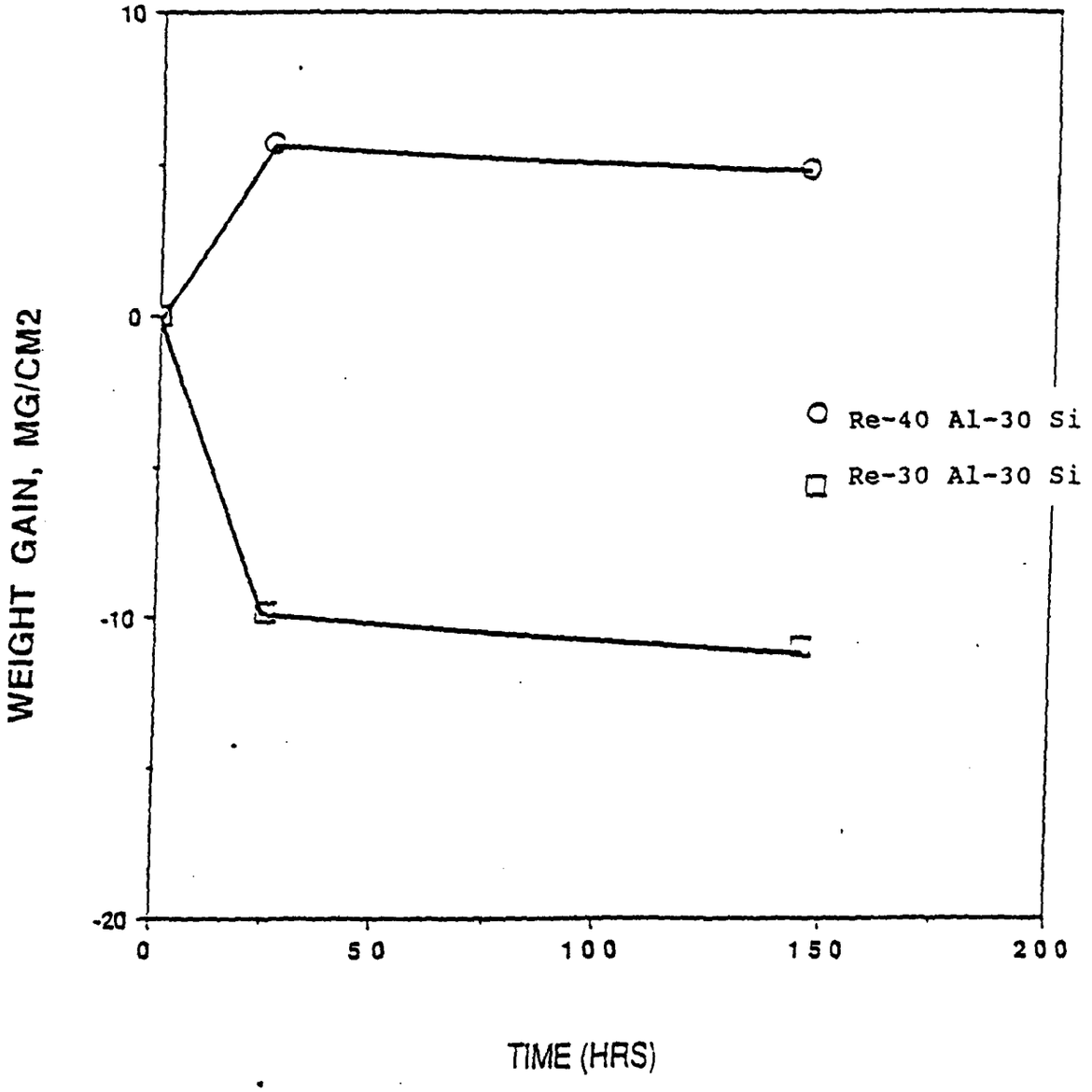

Figure 19. The variation of weight change (WGM) with time for the oxidation of rhenium-aluminum-silicon alloys exposed to 1 atm oxygen at 1,550°C.

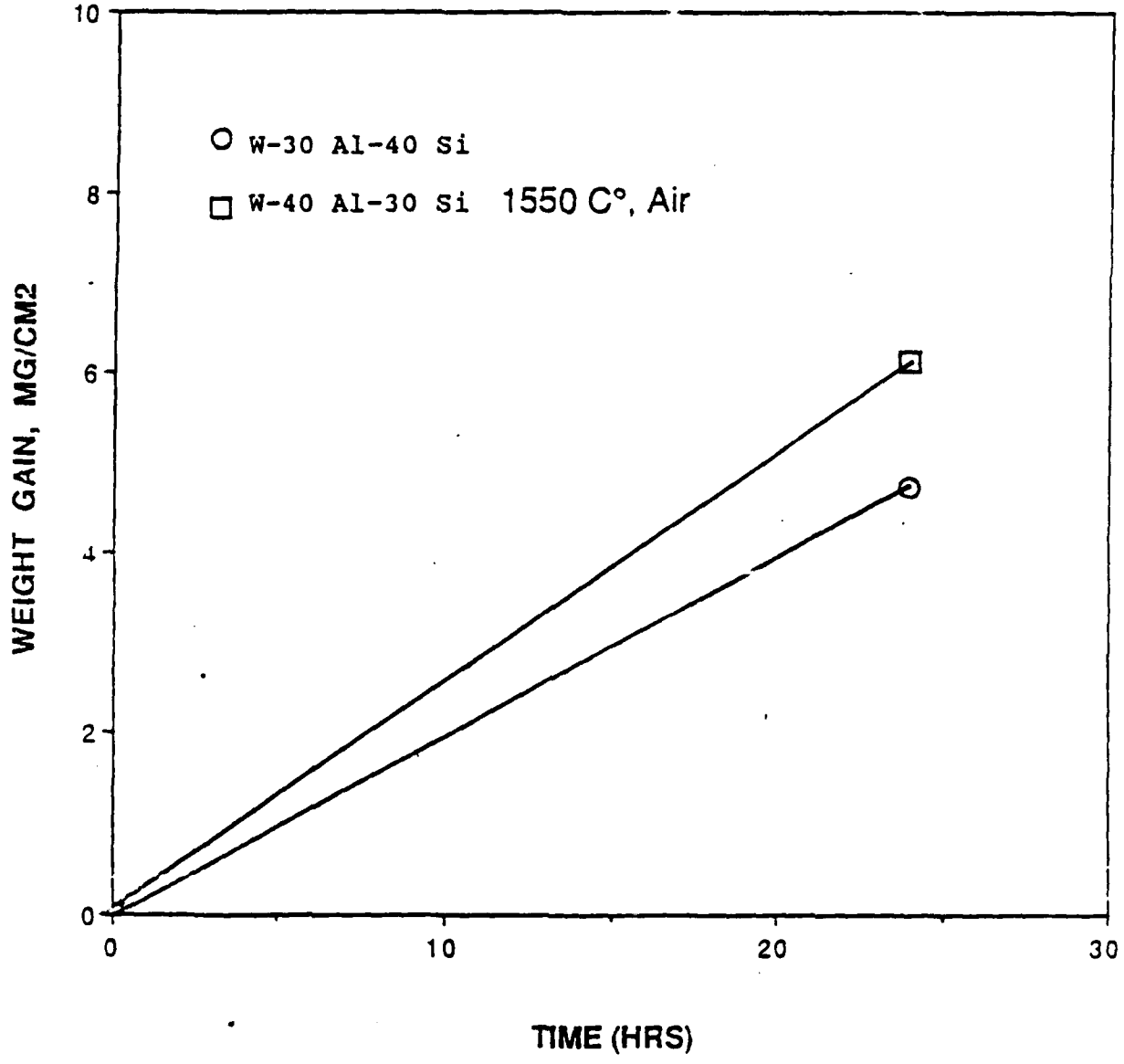

Figure 20. The variation of weight change (WGM) with time for the oxidation of tungsten-aluminum-silicon alloys exposed to air at 1,550°C.

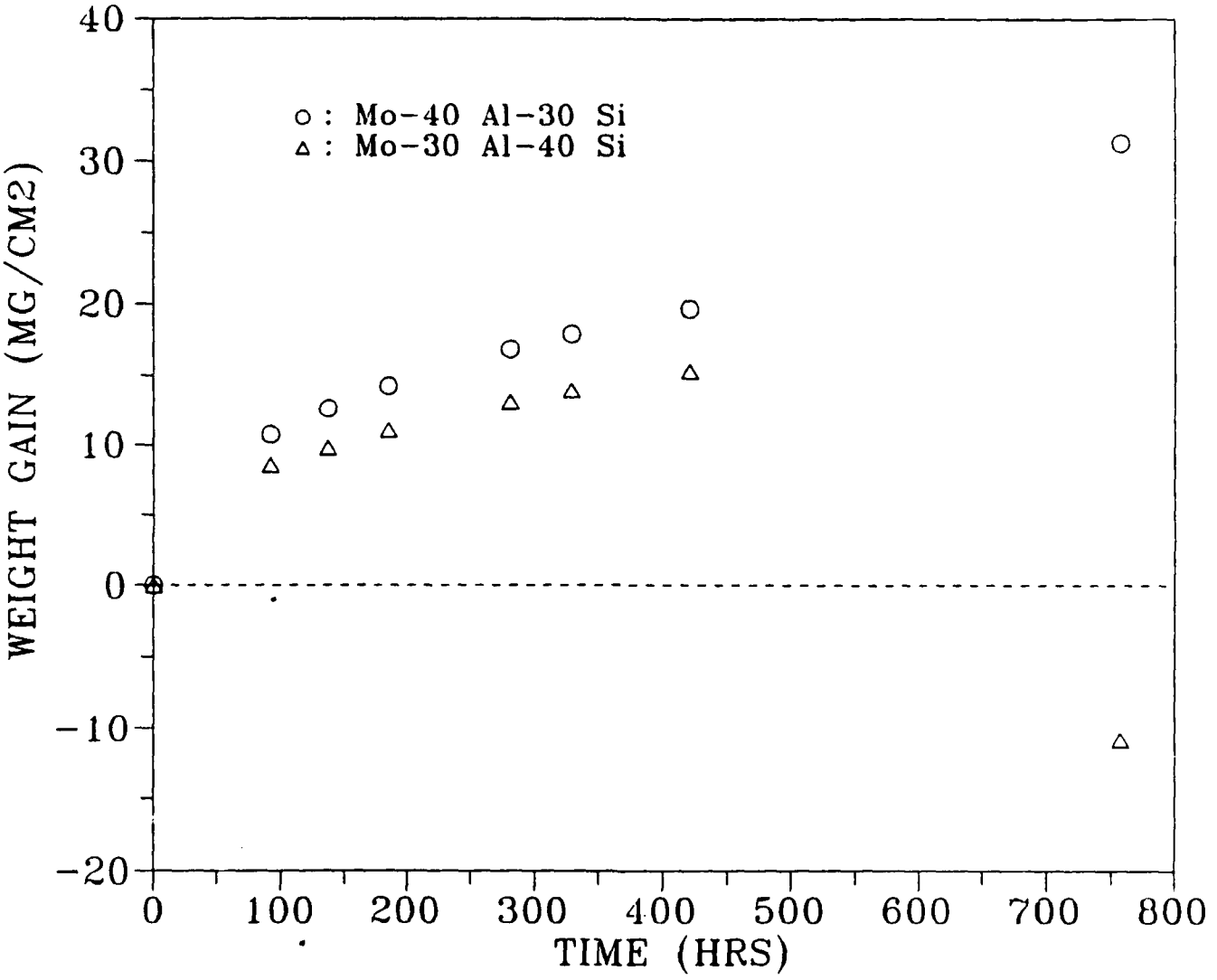

Figure 21. The variation of weight change (WGM) with time for the oxidation of molybdenum-aluminum-silicon alloys exposed to 1 atm oxygen at 1,550°C.

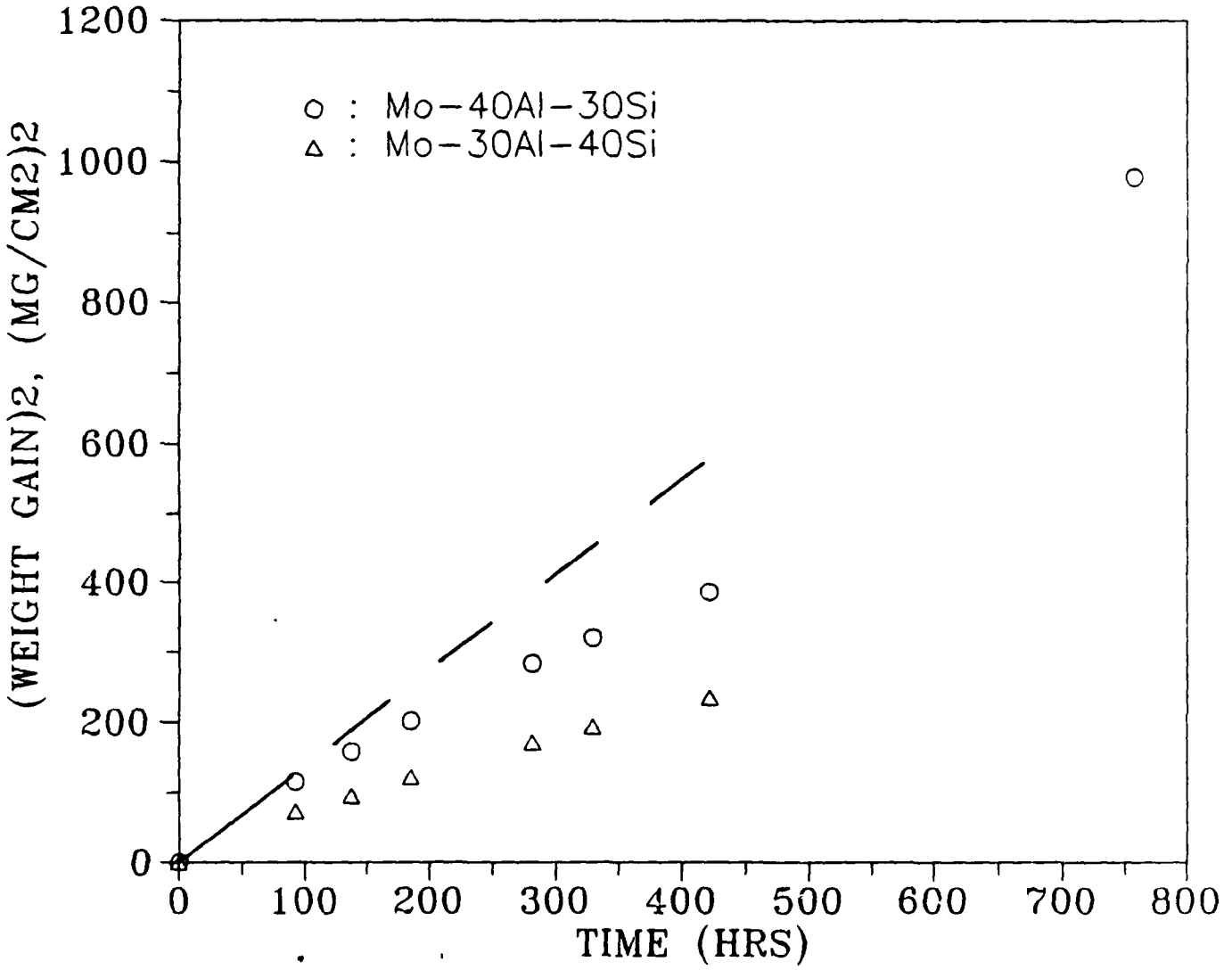

Figure 22. The variation of weight change (WGM) with time for the oxidation of molybdenum-aluminum-silicon alloys exposed to 1 atm oxygen at 1,550°C.

Figures 23.a and 24.a show the cross sections of the oxide scale for the molybdenum-40 aluminum-30 silicon and molybdenum-30 aluminum-40 silicon alloys, respectively, after 800 hours of oxidation in pure oxygen at 1,550°C. As is expected from the oxidation of iridium-aluminum-silicon alloys, no silica is found when the oxide scale is protective (Fig. 23.c), and a layer of silica is found at the inner edge of the alumina scale when the oxide scale has lost its protective nature (Fig. 24.c). The pores, which are observed in these alloys after oxidation, have not been observed in the iridium-aluminum-silicon alloys. In 1 atm oxygen at 1,550°C, the equilibrium pressures of gaseous IrO_3 and MoO_3 are 1.45×10^{-3} and 1.18×10^{7} atm, respectively.[19,21] Thus the pores observed in the molybdenum-aluminum-silicon alloys may be ascribed to the formation of MoO_3 and its extremely high equilibrium pressure.

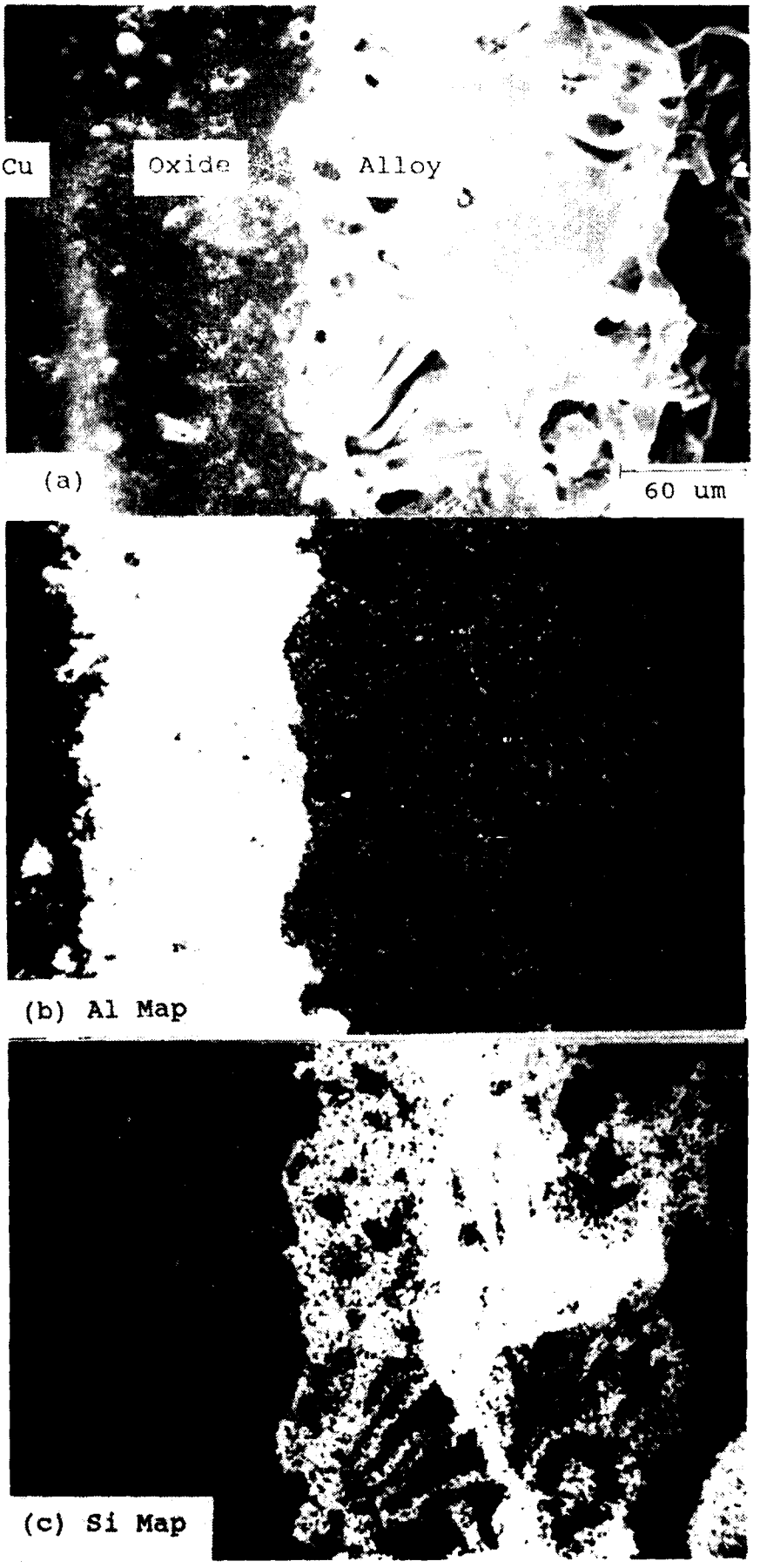

Fig. 23.
Mo-40 Al-30 Si
1 atm Oxygen
800 Hours
T= 1,550°C

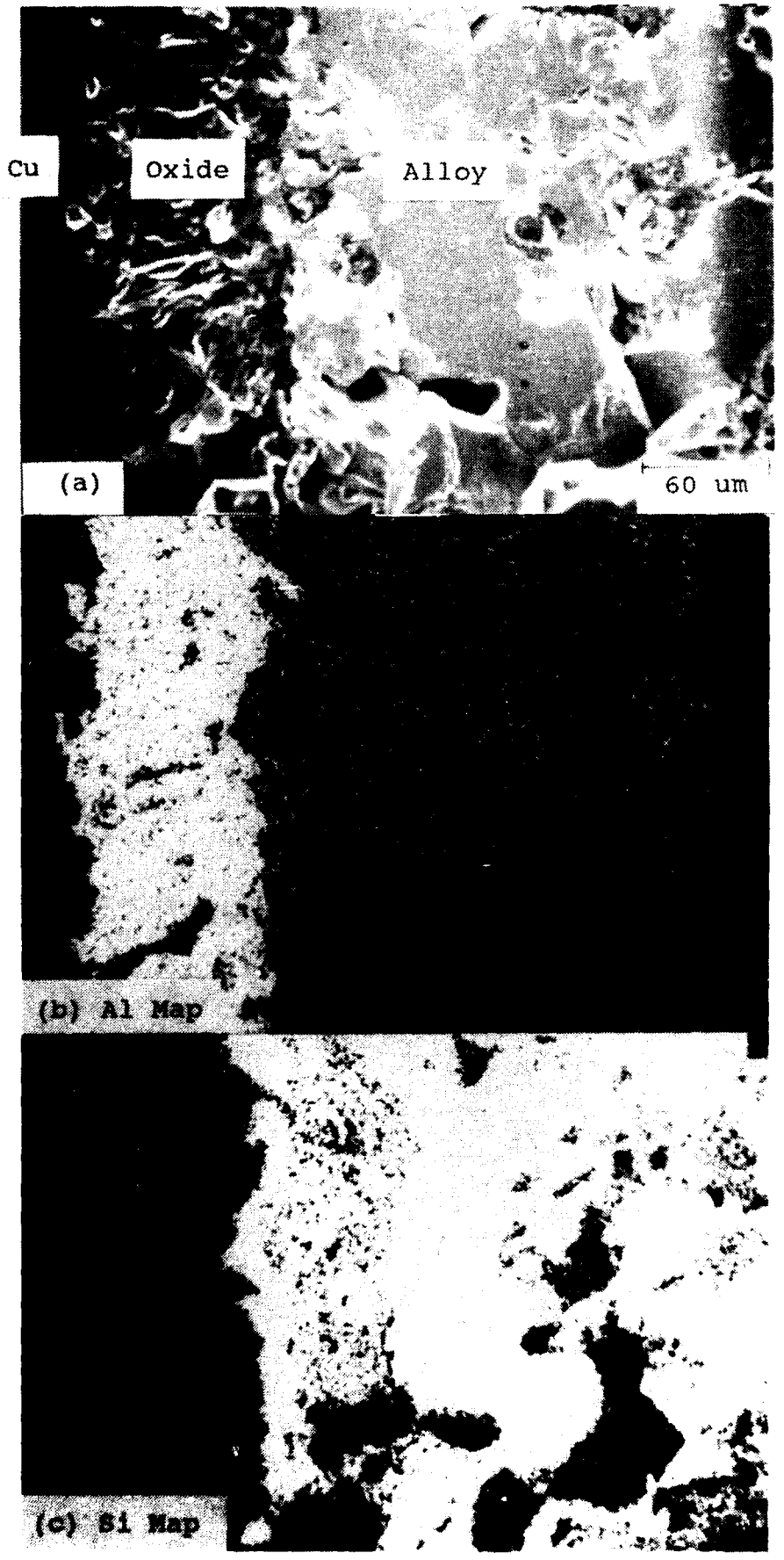

Fig. 24.
Mo-30 Al-40 Si
1 atm Oxygen
800 Hours
T= 1,550°C

IV. SUMMARY

The oxidation behavior of iridium, rhenium, tungsten, and molybdenum-based alloys which were selected as the most promising coating materials for oxidation protection at ultrahigh temperatures has been investigated in 1 atm oxygen at 1,550°C (2,822°F) - 1,800°C (3,272°F).

The hafnium concentration necessary for the formation of a continuous external HfO_2 scale in iridium-hafnium alloys is above 50 at% hafnium. The aluminum concentration necessary for the formation of a continuous external Al_2O_3 scale in iridium-aluminum alloys is above 55 at% aluminum, which is the aluminum-rich boundary of IrAl phase. Thus, it appears that the $IrAl_x$ ($x \approx 2.5$) phase is necessary for the formation of a protective external Al_2O_3 scale on iridium-aluminum alloys. The activation energy for the growth of Al_2O_3 on iridium-60 at% aluminum alloy is in agreement with that determined previously for NiAl at lower temperatures.[1] This suggests that a similar process may control the Al_2O_3-scale growth on these two alloys.

Silicon decreases the aluminum concentration necessary for the formation of a protective alumina scale from around 55 to below 30 at%, and remarkably increases the lifetime of the Al_2O_3 scale. For example, at 1,550°C (2,822°F) in 1 atm oxygen, an iridium-30 at% aluminum-10 at% silicon alloy (20 mils thick) exhibits a protective oxidation behavior for over 300 hours, whereas an iridium-60 at% aluminum alloy (20 mils thick) exhibits a protective oxidation behavior for only about 60 hours. Furthermore, temperature cycling does not lead to scale spallation

or increased oxidation rates. The oxidation behavior exhibits three characteristic stages: initial parabolic oxidation stage, leveled off oxidation stage, and nonprotective oxidation stage. From weight change results and SEM/EDAX analysis, we propose that the oxidation is controlled by the growth of an alumina scale during the parabolic oxidation stage, by the combination of the growth of a silica scale and the loss of gaseous iridium oxides during the leveled off oxidation stage, and by the loss of gaseous iridium oxides during the nonprotective oxidation stage.

We suggest that silicon may increase the aluminum activity in the ternary iridium-aluminum-silicon alloy. The increased aluminum activity will increase the flux of aluminum to the scale/alloy interface and thus decrease the aluminum concentration necessary for the formation of a protective alumina scale. The increased lifetime of the ternary alloys is ascribed to the decreased aluminum concentration necessary for the formation of a protective alumina scale during the parabolic oxidation stage and the formation of silica layer during the leveled off oxidation stage. We propose that the iridium-aluminum-silicon alloys with the aluminum concentration from 30 to 50 at% and the silicon concentration from 8 to 15 at% are the best potential coating materials for substrate protection in oxidizing environments at temperatures above 1,550°C (2,822°F).

Rhenium-aluminum-silicon, molybdenum-aluminum-silicon, and tungsten-aluminum-silicon alloys may also exhibit good oxidation resistance, but the data are too sparse for any definite analysis or conclusions. However, a molybdenum-40 aluminum-30 silicon

alloy exposed to 1 atm oxygen and thermally cycled between 1,550°C and room temperature, exhibits protective oxidation behavior for over 800 hours. Figs. 23.a and 24.a suggest that molybdenum-aluminum-silicon alloys may not be suitable as coating materials for long time applications (several hundred hours) because of the formation of pores in the alloy after long time exposure. We recommend that more work be done for the rhenium, molybdenum, and tungsten-based alloys to fully understand the oxidation behavior.

V. CONCLUSIONS

- The hafnium concentration necessary for the formation of a protective hafnia scale in iridium-hafnium alloys is above 50 at% hafnium.

- The aluminum concentration necessary for the formation of a protective alumina scale in iridium-aluminum alloys is above 55 at% aluminum.

- The growth of a protective alumina scale on iridium-aluminum alloys is controlled by the inward diffusion of oxygen via grain-boundaries.

- Silicon decreases the aluminum concentration necessary for the formation of a protective alumina scale on iridium -aluminum alloys from around 55 at% to below 30 at%.

- Silicon remarkably extends the lifetime of the alumina scale.

- Oxide scale spallation does not occur during temperature cycling of iridium-aluminum-silicon alloys.

- The oxidation behavior of iridium-aluminum-silicon alloys exhibits three characteristic stages: parabolic oxidation stage, leveled off oxidation stage, and nonprotective oxidation stage.

- The controlling mechanism for each oxidation stage is:
  - * Parabolic oxidation stage: Growth of alumina
  - * Leveled off oxidation stage: Growth of silica and loss of iridium
  - * Nonprotective oxidation stage: Loss of iridium

- Iridium-aluminum-silicon alloys with the aluminum concentration from 30 to 50 at% and the silicon concentration 8 to 15 at% are recommended as the best potential coating materials for protection in oxidizing environments at temperatures above 1,550°C (2,822°F).

EFERENCES

1. F.S. Pettit, Trans. TMS-AIME, 239, 1296 (1967).
2. B.H. Kear, F.S. Pettit, D.E. Fornwalt, and L.P. Lemaire, Oxid. Met. 3, 557 (1971).
3. C.S. Giggins and F.S. Pettit, J. Electrochem. Soc. 118, 1782 (1971).
4. F.H. Stott and G.C. Wood, Corros. Sci. 11, 799 (1971).
5. I.A. Kvernes and P. Kofstad, Metall. Trans. 3, 1511 (1972).
6. J.D. Kuenzly and D.L. Douglass, Oxid. Met. 8, 139 (1974)
7. A. Kumar, M. Nasrallah, and D.L. Douglass, Oxid. Met. 8, 227 (1974).
8. E.J. Felten and F.S. Pettit, Oxid. Met. 10, 189 (1976).
9. K.L. Luthra and E.L. Hall, Oxid. Met. 26, 385 (1986).
10. N. Birks and G.H. Meier, Introduction to High Temperature Oxidation of Metals, Edward Arnold, London (1983).
11. P.J. Spencer, O. von Goldbeck, R. Ferro, R. Marazza, K. Girgis, and O. Kubaschewski in: Binary Alloy Phase Diagrams, Volume 2, editor-in-chief Massalski, T.B., American Society for Metals, Metals Park, Ohio, 1986.
12. W.W. Smeltzer and M.T. Simnad, Acta Met. 5, 328 (1957).
13. P. Kofstad, High Temperature Oxidation of Metals, John Wiley & Sons, New York (1966).
14. L. Kaufman, NADC Contract N62269-84-C-0217 Second Annual Review, 1986.
15. Powder Diffraction File, editor-in-chief McClune, W.F., International Center for Diffraction Data, Swarthmore, Pennsylvania, 1984.

16. A. Atkinson, Reviews of Modern Physics, 57, 437 (1985).

17. K.P.R. Reddy, J.L. Smialek, and A.R. Cooper, Oxid. Met., 17, 429 (1982).

18. Y. Oishi and W.D. Kingery, J. Chem. Phys., 33, 480 (1960).

19. E.T. Turkdogan, Physical Chemistry of High Temperature Technology, Academic Press, New York (1980).

20. J.A. Costello and R.E. Tressler, "Oxidation Kinetics of Hot -Pressed and Sintered α-SiC", J. Am. Ceram. Soc., 64, 327 (1981).

21. JANAF Thermochemical Tables, 3rd ed., Edited by M.W. Chase, Jr., C.A. Davies, J.R. Downey, Jr., D.J. Frurip, R.A.McDonald, and A.N. Syverud, National Bureau of Standards, Washington,DC, 1985.

U.S. GOVERNMENT PRINTING OFFICE: 1989-648-056